Biochimica et Biophysica Acta 1777 (2008) 1001–1019

Contents lists available at ScienceDirect

Biochimica et Biophysica Acta

journal homepage: www.elsevier.com/locate/bbabio

Review

The Q-cycle reviewed: How well does a monomeric mechanism of the bc_1 complex account for the function of a dimeric complex?

Antony R. Crofts [a,c,*], J. Todd Holland [c], Doreen Victoria [a], Derrick R.J. Kolling [c], Sergei A. Dikanov [b], Ryan Gilbreth [c], Sangmoon Lhee [c], Richard Kuras [c], Mariana Guergova Kuras [c]

[a] Department of Biochemistry, University of Illinois at Urbana-Champaign, IL 61801, USA
[b] Department of Veterinary Medicine, University of Illinois at Urbana-Champaign, IL 61801, USA
[c] Center for Biophysics and Computational Biology, University of Illinois at Urbana-Champaign, IL 61801, USA

ARTICLE INFO

Article history:
Received 6 February 2008
Received in revised form 26 March 2008
Accepted 23 April 2008
Available online 1 May 2008

Keywords
Q-cycle
Constraints on molecular mechanism
bc_1 complex
Kinetic model
Coulombic interaction
Thermodynamic model

ABSTRACT

Recent progress in understanding the Q-cycle mechanism of the bc_1 complex is reviewed. The data strongly support a mechanism in which the Q_o-site operates through a reaction in which the first electron transfer from ubiquinol to the oxidized iron–sulfur protein is the rate-determining step for the overall process. The reaction involves a proton-coupled electron transfer down a hydrogen bond between the ubiquinol and a histidine ligand of the [2Fe–2S] cluster, in which the unfavorable protonic configuration contributes a substantial part of the activation barrier. The reaction is endergonic, and the products are an unstable ubisemiquinone at the Q_o-site, and the reduced iron–sulfur protein, the extrinsic mobile domain of which is now free to dissociate and move away from the site to deliver an electron to cyt c_1 and liberate the H^+. When oxidation of the semiquinone is prevented, it participates in bypass reactions, including superoxide generation if O_2 is available. When the *b*-heme chain is available as an acceptor, the semiquinone is oxidized in a process in which the proton is passed to the glutamate of the conserved -PEWY- sequence, and the semiquinone anion passes its electron to heme b_L to form the product ubiquinone. The rate is rapid compared to the limiting reaction, and would require movement of the semiquinone closer to heme b_L to enhance the rate constant. The acceptor reactions at the Q_i-site are still controversial, but likely involve a "two-electron gate" in which a stable semiquinone stores an electron. Possible mechanisms to explain the cyt b_{150} phenomenon are discussed, and the information from pulsed-EPR studies about the structure of the intermediate state is reviewed.

The mechanism discussed is applicable to a monomeric bc_1 complex. We discuss evidence in the literature that has been interpreted as shown that the dimeric structure participates in a more complicated mechanism involving electron transfer across the dimer interface. We show from myxothiazol titrations and mutational analysis of Tyr-199, which is at the interface between monomers, that no such inter-monomer electron transfer is detected at the level of the b_L hemes. We show from analysis of strains with mutations at Asn-221 that there are coulombic interactions between the *b*-hemes in a monomer. The data can also be interpreted as showing similar coulombic interaction across the dimer interface, and we discuss mechanistic implications.

1. Introduction

The ubiquinol:cytochrome c oxidoreductase (bc_1 complex) family of redox-linked proton pumps form the core of all major electron transfer chains, with an ancestry dating back to before the great divide. Their importance needs no further emphasis beyond their role in carrying the energy flux of the biosphere. It is generally agreed that a Q-cycle mechanism accounts for the activity of the enzyme, but there are many variants, and which particular variant best explains the finer points is still under debate [1–11]. In the simpler bacterial systems, the kinetic and thermodynamic behavior is well described by the modified Q-cycle [12,13]. This has been discussed extensively in recent reviews [2–5,11,13], and is shown schematically in Fig. 1. The bc_1 complex has a dimeric structure incorporating 4 metal centers in each monomer (hemes b_H and b_L in cytochrome (cyt) *b*, heme c_1 in cyt c_1, and a [2Fe–2S] cluster in the iron–sulfur protein (ISP)), which provide electron transfer chains connecting two quinone processing sites, and three additional catalytic interfaces. Despite this complexity, the mechanism is better understood than that for other respiratory complexes. The oxidation of ubiquinol (QH_2) occurs at the Q_o-site (also

* Corresponding author. Department of Biochemistry, University of Illinois at Urbana-Champaign, 419 Roger Adams Lab, 600 S. Mathews Avenue, Urbana, IL 61801, USA. Tel.: +1 217 333 2043; fax: +1 217 244 6615.
E-mail address: a-crofts@life.uiuc.edu (A.R. Crofts).

0005-2728/$ – see front matter © 2008 Elsevier B.V. All rights reserved.
doi:10.1016/j.bbabio.2008.04.037

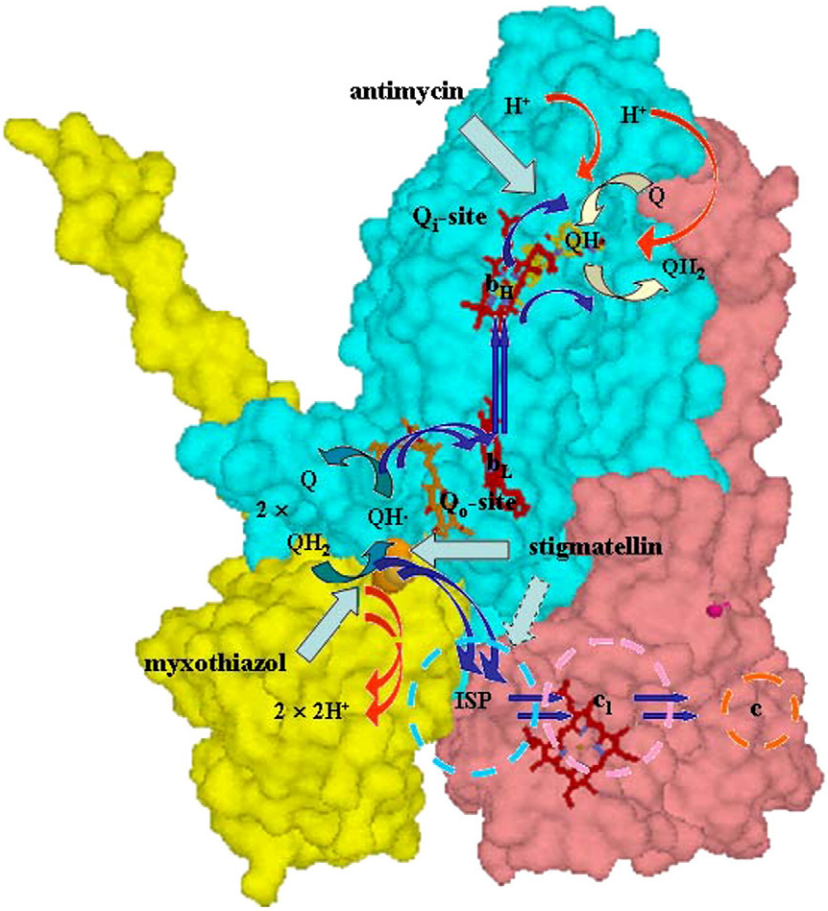

Fig. 1. The modified Q-cycle mechanism. The mechanism demonstrated in the 1980′s, superimposed on the *Rb. sphaeroides* structure (PDB file 2QJK). Electron transfers are shown by blue arrows; H^+ release or uptake by red arrows, exchange of Q or QH_2 by open blue-green (Q_o-site) or yellow (Q_i-site) arrows; inhibition sites by cyan arrows. See text for a description of the operation.

called the Q_P-site), where the two electrons are diverted down two different chains. The first electron goes down the high-potential chain of ISP, heme c_1, and cyt c (or c_2 in bacteria), to an oxidant (a cytochrome oxidase in respiratory chains, or the oxidized reaction center in photosynthetic systems). Removal of one electron leaves a semiquinone (SQ) at the Q_o-site. The second electron is delivered to a low-potential chain of hemes b_L and b_H, which passes the electron on to the Q_i-site (Q_N-site), where it reduces either ubiquinone (Q) to SQ, or SQ to QH_2. Because reduction of Q at the Q_i-site requires two electrons overall, the bifurcated reaction at the Q_o-site has to occur twice to provide these, and to complete a full turnover of the enzyme. The location of the two Q-sites on opposite sides of the membrane gives rise to an electrogenic flux through the low-potential chain, which provides the electrogenic arm, while diffusion of Q and QH_2 across the membrane with oxidation of $2QH_2$ (with release of $4H^+$), or reduction of Q (with uptake of $2H^+$) provides the neutral arms of a Mitchellian proton-pumping loop.

The ancestral history of the bc_1 complex has left an unfortunate mechanistic legacy [14–18]. Oxidation of ubihydroquinone (ubiquinol, QH_2) at the Q_o-site of the complex operates through an intermediate semiquinone (SQ) that has a high reactivity with O_2. This leads to production of superoxide anion, the precursor of reactive oxygen species (ROS) that play havoc with the cellular machinery, and ultimately lead to cellular suffocation through damage to mitochondrial DNA [18,19]. There is some controversy over what fractional contribution this reaction makes to the overall cellular ROS production in humans, but a substantial literature suggests that it may be the major source under some physiological conditions and in some genetic pathologies [20–23]. This design-defect likely reflects an "invention" when the biosphere was anaerobic, and one of the interests in studying the complex has been to see how evolution has subsequently honed the architecture to minimize the effect.

Much of the critical work has investigated the bc_1 complex in *Rhodobacter* species of photosynthetic bacteria. The major advantage of working in photosynthetic systems lies in the fact that the bc_1 complex is tightly integrated into the photosynthetic machinery [24], so that excitation with a saturating flash generates the substrates stoichiometrically, allowing exploration of the kinetics of a single turnover of the intact apparatus on the microsecond time scale. From this work, a detailed description of the mechanism has been proposed, in which the partial reactions have been dissected out, and characterized through kinetic and thermodynamic parameters sufficient to account for the bulk of available experimental data [4,5,25,26]. With the availability of structures [27–33], this physicochemical description has been fleshed out in molecular detail. Although the structures provided strong support for the modified Q-cycle, they also introduced some novel features [34–36]. The structures have also put much detailed work using mutagenesis on a firmer basis, providing insights that have allowed an atomic-level analysis of mechanism.

In this paper, we briefly review recent developments that have provided us with an economical model for turnover in a monomeric complex, and then explore the question whether this is sufficient to explain turnover of the dimer.

1.1. Mobility of the ISP ectodomain

Recognition of the mobility of the extrinsic domain [28] launched a period of controversy about the role of movement of the ISP in control

of function. Much of the speculation has focused on a possible controlling role of such movement. From our own work [36,37], and from Millet's results [38,39] it is clear that movement is always more rapid than the rate-determining step, supporting the interpretation derived from examination of the early structures, which led us to focus instead on specific interactions between the ISP and its reaction partners that may restrict mobility by binding at the reaction interfaces. As we have shown, some of these can be measured directly through thermodynamic effects, and have provided the basis for our models for formation of ES- and EP-complexes [[4,34–36,40]. Some can be observed either through crystallographic solution [28,33,36,41,42], or through spectroscopic studies [42,43]. For many of these complexes, the dominant interaction, either observed directly or proposed, is through H-bonding between *His-161* (bovine numbering is indicated by italics) of ISP and the occupant of the Q_o-site. The nature of these interactions is strongly determined by the protolytic properties of this group, which are also reflected in the redox dependences of the half-cell reactions, and the pH dependence of redox titration data [40,44,45]. We have therefore invested much effort in characterizing these properties, and investigating how they are determined at the atomic level [43,46,47]. Our general approach in this latter investigation has been through specific mutagenesis, thermodynamic measurement (including protein film voltammetry, Table 1), crystallographic solution at high resolution, and detailed spectroscopic investigation of the local protein and solvent environment using pulsed-EPR, Resonance Raman (Fig. 2), and FTIR. Structures at high resolution (<1.5 Å) have been published for wild-type (2NUK) and 5 mutants (2NUM (Y156F), 2NWF (Y156W), 2NVE (S154T), 2NVF (S154C), and 2NVG (S154A) [47]. An additional structure for G133S has been described briefly in the context of spectroscopic data [46]. Five additional structures are at different stages of refinement for mutant strains modified at Leu-132 and Gly-133 (in collaboration with Satish Nair). Our spectroscopic studies have been published in four papers characterizing the WT protein *in situ* in the complex, and as the purified extrinsic domain [43,46,48,49]. Additional work is nearing completion, in which we have dissected the proton environment of the [2Fe–2S] cluster, and identified sites undergoing deuterium exchange, likely involved in H-bonds, and we have similar data from two mutant strains, Y156F and S154A, in each of which we have identified the loss of at least one exchangeable proton, with different properties in the two mutants. From the two structures for mutant strains at these different sites already published, we can say with confidence that the structures are essentially unchanged except for the loss of a single H-bond resulting from the mutation. It follows that the changes in thermodynamic and kinetic properties must arise from this change. For both mutations (Y156F, S154A), DFT/electrostatic calculations have recently been performed [50], and the results were in good agreement with our experimental data (Table 1), and support previous speculation [51–53] as to the importance of these interactions. From this extensive work we now have a detailed picture of the structural underpinnings of the thermodynamic properties of the ISP, and a much clearer understanding of how these properties are modified by mutation. At the resolution provided by our structures [46,47], crystallography provides true atomic-level positions for all non-H atoms, and in some cases also shows electron density for H-atoms. For some H-bonds, this makes it possible to identify angular parameters. This information is also in principle available from pulsed-EPR data. The special interest of our studies lies in the fact that we are accumulating such data from the same set of proteins, which will allow a cross-validation of methodologies. Our recent observation that the backbone –NH of Leu-132 provides a H-bond to S2 of the cluster, and that the geometry leads to significant spin density on the N-atom (and by extension, on the S-atom of the cluster) is a nice demonstration of the synergy between these approaches [46].

1.2. Q_o-site reaction

From our earlier studies relating Berry's first complete structures to function, we had suggested a scenario in which movement of the extrinsic domain of the ISP was a spontaneous diffusional process with an expected time scale in the sub-microsecond range [28,35,36]. We demonstrated the feasibility of this scenario through molecular dynamic simulations. We pointed out that binding processes at the catalytic interfaces were likely relatively weak, based on the previously measured kinetic constants, and expected collision-limited rates, and on the occupancy of ISP in structures. In a more recent extended series of kinetic measurements [37], we were able to confirm these expectations, and demonstrate limits on reaction rates which were in line with these earlier speculations. These measurements provided a number of useful constraints on the mechanism.

a) We demonstrated that the oxidation of QH_2 in the absence of antimycin, determined from the electrogenic events associated with turnover, occurred at the same rate as that in the presence of antimycin, determined from the rate of reduction of heme b_H [37]. This result was important because it precluded any mechanisms in which physicochemical properties affecting turnover at the Q_o-site were modified by binding of antimycin at the Q_i-site (cf. [9,10,53]).

b) We analyzed the rates of partial processes in the high-potential chain, and compare these with the turnover of the Q_o-site as determined by the kinetics of reduction of heme b_H in the presence of antimycin. We demonstrated that the 120 μs lag before onset of heme b_H reduction was almost all accounted for by the time needed to get an oxidizing equivalent to the Q_o-site. This result was important because it placed constraints on the movement of ISP, and on the stoichiometry of intermediate states, including that of the SQ. Since the rate-limiting step

Table 1
Electrochemical parameters measured by CD spectrum, protein film volatammetry, and kinetic titration

Strains	E_m values from CD spectra (mV)	Protein film voltammetry					Kinetic titration at 83% reduced quinine pool[d]		
		E_{acid} (mV)	E_{base} (mV)	pK_{ox1}	pK_{ox2}	p$K_{red1,2}$	pK_A	pK_B	V_{opt}
Wild-type/BH6[a]	303±4[b]/312±5[c]	308±3	−134±6	7.6±0.1	9.6±0.1	12.4±0.4	6.66±0.10	9.14±0.26	973.3
S154T	260±5[b]	288±3	−151±7	7.71±0.14	9.32±0.15	12.2±0.1	6.83±0.12	8.48±0.14	826.1
S154C	313±5[b]	324±4	−97±6	7.17±0.11	9.77±0.13	12.0±0.1	6.29±0.05	8.46±0.06	804.0
S154A	167±6[b]	178±4	−239±10	8.06±0.15	9.89±0.17	12.5±0.1	7.52±0.20	10.2±0.28	199.2
Y156F	256±4[c]	252±4	−165±6	7.76±0.15	8.83±0.21	11.8±0.1	6.90±0.06	8.54±0.08	714.6
Y156W	198±3[c]	208±3	−228±4	7.87±0.09	9.25±0.11	12.2±0.1	6.97±0.08	9.69±0.12	242.7

[a] The wild-type strain in this work is a complementary mutant strain of *Rb. sphaeroides* BC17, which contains the pRK415 with a modified *fbc* operon which has a histidine-tag at the C-terminus of the cyt *b* gene. The protein film voltammetric data of the wild-type was reported [44].

[b] The values are measured at pH 7.4.

[c] The data represent the limiting value for E_m at pH ≪pK_1, as described in [59].

[d] V_{opt} is the optimal reaction rate achieved when the first protonable group is deprotonated (pK_A) and the second group is protonated (pK_B), according to the following equation from the reference [148]. $v = V_{opt} \cdot \left(\frac{K_A}{K_A+[H^+]}\right)\left(\frac{[H^+]}{K_B+[H^+]}\right)$.

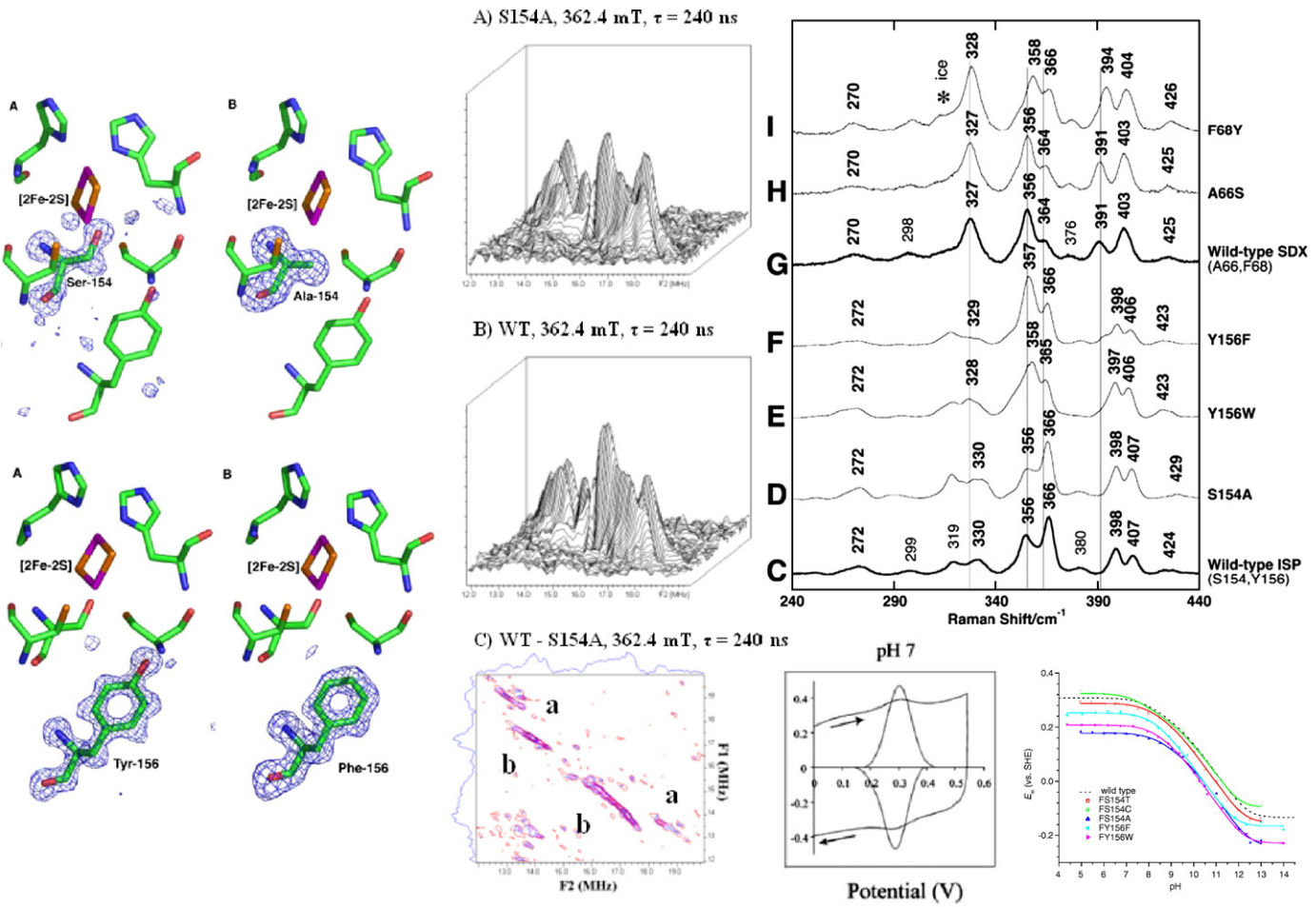

Fig. 2. Synergy of spectroscopy, crystallography, and thermodynamic analysis. (Left) Structures of wild-type, S154A and Y156F mutants (modified residues shown with electron densities); (middle) 2D ESEEM plots showing proton profiles in wild-type and S154A, and difference (bottom), showing loss of protons a, b (similar data have been obtained for the Y156F mutant); (right) RR spectra showing differences in ISP mutants S154A and Y156F, compared to SDX mutants and wild-type, and (bottom) PFV titrations, showing voltammogram (left, WT, pH 7), and E_m vs. pH curves from titration data for wild-type and five mutant strains (right).

was identified as the first electron transfer, with a rate constant of ~770 μs, the unaccounted lag of <20 μs would limit any occupancy to <0.026 for any intermediate between QH_2 and heme b_H [37]. This constraint on occupancy can be lowered to <0.015 on the basis of work from Millett's lab in which the reaction was initiated in the isolated *Rb. sphaeroides* complex by flash activation via a bound ruthenium complex [39,54]. This result eliminates all reaction mechanisms in which a stable (K>0.015) SQ-ISPH intermediate is required [55,56].

c) For the Q_o-site reaction itself, the first electron transfer (to ISP_{ox}) had been identified as the rate-determining step in QH_2 oxidation on the basis of dependence on driving force [25,26,57–59]. We had proposed a specific role for the H-bond between *His-161* of ISP, and either QH_2 as H-bond donor in formation of the ES-complex, or Q as H-bond acceptor in formation of the EP-complex [25,40,45,59,60]. The difference between these roles depended on the protolytic properties of the histidine. We suggested that this group was responsible for the pK at 7.6 measured on the oxidized ISP. This pK was shifted to >12 in the reduced form. From this hypothesis, several predictions could be made about the properties of the first electron transfer reaction. The predictions were framed in the context of a mechanism in which the transfer of an electron (together with a proton) from QH_2 to ISP_{ox} occurred in a strongly endergonic process to generate the intermediate SQ at low occupancy. From the structures, and our proposal for the nature of the ES-complex, several paradoxical features had to be explained. These related to the high activation barrier, the slow rate of the overall reaction, and the very short distance for electron transfer (~7 Å). Since, after reduction, the ISP would be protonated, the reaction effectively involves H-transfer in a proton-coupled electron transfer. In the treatment proposed [4,40,42], the pK of *His-161* contributed two separate effects. The first of these involved the role of the dissociated form of ISP_{ox} in formation of the ES-complex, in which QH_2 was the H-bond donor in the complex with ISP_{ox}. This meant that the concentration of ISP_{ox} as a substrate was determined by the pK on *His-161*. We demonstrated that this was the case by measurement of the pH dependence of electron transfer, which showed Michaelis–Menten saturation for ISP_{ox} [25]. Support for this interpretation was provided by use of a mutant ISP (Y156W) with a shifted pK, which also showed a corresponding shift in pH dependence [59]. The second effect of the pK on ISP_{ox} came from its role in determining the energy level of an intermediate proton configuration [61]. We suggested that electron transfer proceeded from an unfavorable configuration of the H^+ in the H-bond, determined by a Brønsted relationship and the pK values for QH_2 and ISP_{ox}. The reaction interface was anhydrous, so this necessitated a proton-coupled electron transfer along the H-bond. We pointed out that the unfavorable intermediate state would contribute part of the energy barrier determining the rate of electron transfer, and that this could explain the observed properties. A detailed Marcus-type analysis showed that the behavior of WT could be accounted for economically by this mechanism, and the same treatment also explained the behavior of a set of mutant strains with modified E_m and pK values for ISP [4].

Because of the important role of the p*K* on *His-161*, and the coupling between redox and protolytic properties, we have invested much effort in determining the structural basis of these properties (see above). The attribution of the p*K* to a liganding histidine has now been confirmed by spectroscopy [62–64] and computational modeling [50] (see above). The mechanism proposed successfully accounts for the properties of the first electron transfer. Since this is the rate-determining step, our detailed mechanism in the context of the modified Q-cycle also explains much of the subsequent behavior of the complex.

d) We had proposed that the second electron transfer at the Q_o-site might require a movement of the SQ from a location in the site distal from heme b_L where it was generated on oxidation of QH_2 to a proximal location, allowing ~1000-fold enhancement of rate constant and rapid reduction of the heme at low occupancy [25,60]. We had suggested a role for the conserved glutamate (Glu-295 of the -PEWY-span), which acted as a second H-bonding residue involved in formation of the ES-complex [34]. In this mechanism, oxidation of QH_2 by H-transfer to ISP_{ox} would generate the $QH^{\bullet}$ form of SQ. Glu-295 would facilitated H^+ released by accepting a H^+ from $QH^{\bullet}$, and rotating to deliver the H^+ to a water chain leading to the exterior, leaving Q^- as the mobile form. Hunte et al. [8,65] have adopted a similar mechanism based on their yeast bc_1 complex structure, which was the first to show the water chain we had suggested from MD simulations [36]. More recently, Osyczka et al. [1,7] discussed possible mechanisms for the prevention of bypass reactions. They concluded that none of those previously proposed would work, because any configuration of the site allowing occupancy by SQ under circumstances in which heme b_L was reduced would give bypass rates similar to forward rates. We demonstrated that the alternatives discussed by them where physicochemically unrealistic, but that our earlier mechanism could function both to allow rapid forward electron transfer, and to limit bypass reactions by a coulombic gating [3,5]. We showed that the behavior of strains in which Glu-295 was mutated were consistent with the mechanism proposed. However, we should note that several other groups have constructed similar mutations in other systems, and although the results are for the most part consistent between groups, the interpretations have provided a different gloss on mechanistic aspects 66–68]. This residue is not absolutely conserved, and none of the mutants is completely inhibited, and some (for example E295D) show rates as high as 20% wild-type, and these facets have been interpreted as showing that Glu-295 is not mechanistically important. Our own analysis of bypass reactions clarified the arguments of Osyczka et al. [1,7], rejected their main conclusions, and provided severe constraints on possible mechanisms. The coulombic gating mechanism proposed involving Glu-295 offered a novel and successful resolution to the paradox they uncovered. A different gating mechanism was suggested by Mulkijanian [9], with alternative proton exit pathways, but a similar role for the glutamate. A role for glutamate in proton exit has been supported by the results of electrostatic calculations of different conformers at the Q_o-site [69]. However, the site involves a metastable ES-complex, and because transitory states were not included in the calculations (which considered only the fully reduced or oxidized complex), the results can only be taken as providing an indication of potential protonation changes coupled to thermodynamically accessible states.

The question of the role of SQ in the Q_o-site reaction has been controversial for many years. Suggested mechanisms have ranged widely, from expectations for a major fraction of centers occupied by SQ in the intermediate state [31,55], through low occupancy models [25,26], to scenarios in which no SQ was expected [1,7]. In addition to the properties that led us to favor a low occupancy model [4,5,25], two other lines of evidence have strongly supported our suggestion that the SQ intermediate is formed at low occupancy by an endergonic proton-coupled electron transfer. Forquer et al. [70], in studies of bypass reactions and super oxide (SO) formation, have confirmed that in yeast, as in the *Rb. sphaeroides* complex, the rate of the first electron transfer is determined by driving force (and is therefore the limiting process), and have shown that the normal forward reaction, and the formation of SO both have the same activation energy. Secondly, Cape et al. [71] have demonstrated that SQ is formed at the site at low occupancy (~0.01) under anaerobic conditions in the presence of antimycin. Zhang et al. [72] have also demonstrated a SQ signal with a different line shape, also under anaerobic conditions, in a mutant truncated so as to remove heme b_H, so that in each case electron transfer out of the *b*-heme chain was prevented. Each of these observations is consistent only with the second of these models. Cape et al. also showed that the SQ is not in H-bonding contact with any N-atoms (excluding a complex with ISP), but was in a constrained environment (assumed to be the Q_o-site volume), as expected from the Hong et al. [25] mechanism. The occupancy of SQ was at the high end of the range expected from the rate of bypass reactions, but the occupancy expected was based on an assumed reaction distance similar to that in the ES-complex. The appearance of SQ was not time resolved in either of these studies. However, it is clear from the very low rate of bypass reactions under normal forward electron transfer that the re-oxidation of SQ keeps the level much lower than this [5], and it seems probable that SQ appearance in these experiments required reduction of the *b*-heme chain by one or more turnovers of the Q_o-site before SQ could accumulate. This is likely also the explanation for the discrepancy between the results above [71,72] and the observation of Zhu et al. [73] in which no SQ was observed on initiation of turnover of the oxidized bovine complex by QH_2 addition. The authors make no mention of redox conditions, but the complex was initially fully oxidized and no antimycin was added, and it seems likely that the conditions were aerobic. Under aerobic conditions Cape et al. did not see SQ, in line with previous reports [26,74], and attributed this to reaction of SQ with O_2. The failure of Zhu et al. [73] to observe SQ could therefore be attributed to either its oxidation by O_2, or rapid re-oxidation by heme b_L, and is as expected from all these prior reports. Zhu et al. [73] reported the kinetics of reduction of heme b_L and ISP, and also showed raw data indicating the reduction of heme b_H and the appearance of SQ at the Q_i-site. For ISP and heme b_L, 10% of the signal showed matched rates of reduction with $t_{1/2}$ ~200 μs. This half-time might imply a rate ~4-fold faster than the fastest rates previously reported in native photosynthetic membranes [25], or in the isolated complex [54], from *Rb. sphaeroides*, and ~25-fold faster than rates of Q_o-site turnover measured by stopped-flow in the isolated bovine complex in the presence of antimycin. Taken at face value, the rapid and matched rates of reduction of ISP and heme b_L might be thought to place more severe constraints on the possible occupancy of SQ at the Q_o-site than those previously suggested [5], but the noise level apparent in the EPR data shown would preclude more quantitative estimation. One possible explanation for the initial kinetics seen by Zhu et al. [73] is that the initial reaction represents a reduction kinetics truncated by re-oxidation, since the complex was initially fully oxidized. Indeed, extrapolation of the initial rate shows 50% completion at 1.1 ms, suggesting that the initial rate was in line with that measured previously for the rate-limiting first electron transfer reaction. If this is the case, and if a mechanism limited by the first electron transfer is assumed, the new data provide no tighter constraints than those previously estimated (see discussion above and [5,26,39,54]). The lower range of plausible occupancies calculated was ~10^{-8} SQ/site [3–5,25], and such levels are certainly not precluded by the Zhu et al. [73] results. Any estimate of occupancy less than the previously calculated upper limit would make it more imperative to account for the rapid overall rate observed in terms of a rate constant for the second electron transfer faster than that possible if SQ had to react from the distal domain of the Q_o-site [5]. No kinetic data in the presence of antimycin were reported by Zhu et al. [73], although effects of antimycin addition were discussed. De Vries et al. [75] had shown a faster rate of cyt b_H reduction in the absence than in the presence of antimycin, which was insensitive to myxothiazol, but the

data reported by Zhu et al. suggest a delayed reduction of heme b_H and a simultaneous appearance of SQ in the absence of antimycin.

1.3. Mechanism of the Q_i-site

Any mechanism must account for the fact that the Q_i-site operates as an interface between the 1-electron chemistry of the *b*-heme chain, and the 2-electron chemistry of the quinone pool, and involves intermediate states tuned to binding of the three components of quinone redox chemistry, Q, SQ and QH_2. Since the liganding requirements for these differ markedly, the site must be reconfigured during the catalytic cycle to accommodate these different requirements. In addition, pathways for uptake of two protons and for exchange of substrate and product need to be identified. It is generally supposed that the site operates through a two-electron gate in which heme b_H reduces Q to SQ on one turnover of the Q_o-site, and SQ to QH_2 on a second turnover [12,24].

1.3.1. The two-electron gate at the Q_i-site

The reaction at the Q_i-site has been treated as a simple two-electron gate [24]. However, it has long been recognized that even such a simple treatment has built-in complexities relating to the involvement of three different components, Q, SQ and QH_2, as binding partners. The site has to accommodate each of these in any catalytic cycle, and each has its own requirements in terms of H-bonding [76]. The paradigm for discussion favored in the literature is in terms of the disproportionation reaction [77,78]. Values for the differential binding of Q and QH_2 and SQ stability are based on analysis of titration data from the EPR measurement of SQ. However, a disproportionation is clearly not appropriate as a description of the catalytic cycle, because, on the time scale of turnover, the site can only accommodate one species at a time, and the SQ is not exchangeable. Alternative approaches have been suggested, which attempt to reconcile the SQ data with the properties of the high-potential form of heme b_H associated with the cyt b_{150} phenomenon [79–81]. Our recent efforts on the Q_i-site have been directed at the construction and characterization of mutant strains, and exploration of the local protein and solvent environment of the SQ form, since this information is accessible though pulsed-EPR [76,82–85. These have provided a detailed picture of the local structure [76,84], which, together with the available crystallographic data [41,65,86,87], has allowed new insights to mechanism. The pattern of H-bonding interpreted from crystallographic data has varied between labs. Berry's structures of the bovine and chicken mitochondrial complexes have shown a conserved *His-201* and *Asp-228* as ligands to carbonyl O-atoms of a bound quinone species, and the most recent structures of the *Rb. sphaeroides* complex from Xia's group, have also shown a direct ligand from the equivalent His-217. In structures of the yeast mitochondrial complex from the Hunte group, the H-bond to the histidine has been through a water molecule. In structures of mitochondrial complexes from Xia and collaborators, both H-bonds are modeled as through waters. Several of these structures are at close to atomic resolution, but because the quinone present can become reduced to SQ by X-ray exposure [88,89], the nature of the occupant in these structures is ambiguous. Our own EPR results are interpreted as showing ligands equivalent to those seen in Berry's structures (His-217 and Asp-252). However, MacMillan (personal communication) has reported that the N_ε of histidine seen in our ESEEM spectra is not visible in his using the yeast complex. The difference may come from the protocol used for generation of the SQ, — reduction by ascorbate at pH 7.8–9.0 in our experiments, and by dithionite at pH 9.5 in MacMillan's. The discrepancies between labs might also provide clues about variability in liganding of the three species occupying the site during catalytic turnover, and variability with pH on dissociation of liganding sidechains [76,84], but we have not yet explored all these possibilities. Our conclusions are summarized in a scheme in which conformational plasticity allows the site to reconfigure to adapt to the binding requirements of the bound Q, SQ, and QH_2 forms that participate in the reaction [76]. It is likely that the primary ligands, His-217 and Asp-252, act as proton exchange sites; His-217 lies at the surface, so it provides a direct pathway, but Asp-252 is quite buried. Electrostatic calculations on the yeast complex suggest a strong coupling between residues equivalent to Asp-252 and Lys-251, other nearby lysines in cyt c_1, and possibly bound cardiolipin. These are suggested to provide a channel for proton exchange with the aqueous phase [69].

Our more recent efforts have involved experiments to explore the N-environment, and the possibility of a third H-bond from Asn-221 (equivalent to Ser-205) [90]. In our previous work, no spin density on any additional N-atom apart from the histidine N_ε could be detected using ^{14}N X-band. From the ^{14}N S-band and ^{15}N X-band spectra, we have now determined the complete nuclear quadrupole tensor of the ^{14}N, and the isotropic and anisotropic couplings, with the N_ε of His-217. However, no significant spin density on other N-atoms was detected. DFT calculations showed that the energies expected from the Asn-221 H-bond would be masked by the dipole–dipole signals from other N-atoms, leaving the question open. Several mutant strains at Asn-221 were constructed, were able to grow photosynthetically, and showed turnover of the Q_i-site reactions, but with inhibition in rate, and modified properties for heme b_H. We therefore concluded that the potential H-bond from Asn-221 is not essential, but is important for function. The characteristics of the weak H-bond observed through exchange with deuterium suggest that it involves a bound H_2O, but some of the diagonal peaks in ^{15}N HYSCORE spectra could have been contributed by a H-bond from Asn-221. The most recent structures [87] include one showing a quinone occupant (PDB ID 2qjy), in which N_ε of His-217 serves as a direct H-bonding ligand, as seen by EPR [90], no H-bond from Asn-221, and a distance to Asp-252 too great for a direct H-bond, but compatible with a water-mediated H-bond. The structure most likely reflects the occupancy by the oxidized Q.

1.3.2. The role of cyt b_{150} in the mechanism of the Q_i-site

The component known as "cyt b_{150}" is due to a perturbation of the properties of a fraction of heme b_H on interaction with SQ at the Q_i-site. It is seen in redox titrations of chromatophores [91], mitochondria [92] or isolated complexes [93], as a component titrating with $E_{m,7}$ 150 mV only in the absence of antimycin [81]. From the properties of cyt b_{150} we suggested that the Q_i-site catalyzes the following reaction, in which the cyt b_{150} is represented by the state cyt $b_H H\,Q^{\cdot-}$ [2,94]. The reaction (Eq. (1)) can be considered as a reversal of the normal forward reaction by which ferroheme b_L reduces SQ to QH_2, and, after release of the product, binds Q to re-establish the starting state for the Q_i-site.

$$QH_2(\text{pool}) + \text{cyt } b_H Q \leftrightarrows Q(\text{pool}) + \text{cyt } b_H H\,Q^{\cdot-}(H^+) \quad (1)$$

This overall reaction can be split into partial processes:

$$QH_2(\text{pool}) + \text{cyt } b_H Q \leftrightarrows Q(\text{pool}) + \text{cyt } b_H QH_2 \quad (1a)$$

$$\text{cyt } b_H QH_2 \leftrightarrows \text{cyt } b_H H\,Q^{\cdot-}(H^+) \quad (1b)$$

allowing definition at any defined pH, of an equilibrium constant for formation of the cyt b_{150} form:

$$K_{eq} = K_{(1a)}K_{(1b)} = (K_{A(QH2)}/K_{A(Q)})\exp((E_{m(cytbH)} - E_{m(QH\cdot/QH2)})F/RT)) \quad (2)$$

where K_A values are association (binding) constants for QH_2 and Q, and $E_{m(cytbH)}$ and $E_{m(QH\cdot/QH2)}$ refer to the mid-point potentials of cyt b_H, and of the SQ/quinol couple bound at the site, respectively.

The affinities for Q and QH_2 can be subsumed under the terms for the potential of the quinone pool and the Q/SQ couple at the site, since

the ratio of binding constants for Q and QH_2 contributes to the value for $E_{m(QH\cdot/QH2)}$ so as to cancel the ratio of binding constants. This gives:

$$K_{eq} = \exp((E_{m(cytbH)} + E_{m(Q/QH\cdot)}) - 2E_{m(Qpool)})F/RT \quad (3)$$

(where $E_{m(Q/QHP)}$ refers to the bound couple), which can also be derived directly from Eq. (1). A computer model based on this set of equations allows exploration of the variation of redox states of all components as a function of redox potential, pH, etc. In this treatment, no account is taken of different protonation states, local coulombic effects, etc., and these effects are subsumed under existing terms. However, the observed pH dependence of both the b_{150} and SQ titrations are handled by a single p*K* value, currently assigned to SQ (see discussion below).

The mechanism proposed here is in contrast to the mainstream of discussion which starts from consideration of the disproportionation reaction as a basis for mechanism [77,82,95,96]. Since structures became available, there has been little discussion of how this might occur at a site that appears too small to contain more than one species. The Q_i-site catalyzes a quinol–quinone transhydrogenase reaction that allows transfer from exogenous quinol to bound quinone, or between exogenous quinones [97,98]. A plausible mechanism would be for two electrons from a donor Q_dH_2 to be stored in the two *b*-hemes, allowing dissociation of the Q_d, and its replacement by an acceptor Q_a, which would then leave the site as Q_aH_2 [98]. The rate of such a reaction would depend strongly on the probability of populating the $b_H^- b_L^-$ state. The unfavorable equilibrium constant for reduction of heme b_L through b_H [12,99] would account for the relatively slow rate observed. Nevertheless, this would likely be sufficient to allow equilibration on the time scale of a redox titration. Equilibration through 1-electron transfer processes might also occur through direct or indirect interaction with mediators. Since the conditions used to assay semiquinone by EPR (high concentrations of redox mediators, and a long equilibration time) would allow the reaction to reach equilibrium, it is reasonable to use the data in discussion of mechanism, but it is highly unlikely that it reflects the kinetically important intermediate states.

Since the hemes are 1-electron acceptors, it is necessary to take account of the equilibration of the Q/QH_2 couple with heme b_H through 1-electron transfer reactions, — an attractive feature of the cyt b_{150} mechanism proposed. Reduction of heme b_H through the Q_i-site by exogenous quinones, with generation of a semiquinone, occurs on addition of quinol substrate to the oxidized complex in the presence of myxothiazol. In a definitive study by de Vries [75], reduction by duroquinol led to generation of ferroheme b_H and SQ simultaneously, with the reaction ~90% complete at the first point of measurement at 5 ms (using 300 μM QH_2). From this, a value of $\tau < 3$ ms seems appropriate. In chromatophores, where the reactions using the native substrate can be followed *in situ*, the myxothiazol insensitive reduction of heme b_H on generation of 1 QH_2 in the oxidized pool also occurred with $\tau \sim 3$ ms [80]. Since this is ~two orders of magnitude faster than the transhydrogenase reaction, the disproportion reaction is excluded. It seems likely that duroquinol, and presumably other quinols, can react directly and rapidly at the Q_i-site by exchange with the initial occupant.

Rich et al. [96] have discussed the cyt b_{150} phenomena in terms of differential affects of occupancy by Q, SQ or QH_2 on the E_m of heme b_H (see also [82]). A set of 7 different E_m values and 2 p*K*s was required to account for the properties of both the SQ and cyt b_{150}, but these parameters did not include the possibility for differential binding of the different components. Furthermore, in deriving this set, Rich et al. [96] had to assume that SQ generated in the presence of oxidized heme b_H was EPR silent due to magnetic quenching (see also [100]). If the semiquinone signal at the Q_i-site is modulated by magnetic interaction with the spin of oxidized *b*-heme [100,101], this would lead not only to loss of amplitude, but also to some displacement of the maximum of the bell-shaped titration curve [96], and hence to misleading values for derived thermodynamic parameters. There is no doubt that occupancy by inhibitors can modify properties of heme b_H, and a substantial literature showing changes in both E_m and λ_{max}, but the complexity of the Rich et al. treatment makes it somewhat intractable to testing. In contrast, the model proposed here has only a single equilibrium constant, and singular E_m values for heme b_H and the quinone system taken directly from experiment. Computational modeling shows that the properties of the cyt b_{150} phenomena are reproduced quite well using measured values for E_m for heme b_H, values for binding constants and E_m values for the $Q/SQ/QH_2$ system derived from redox titrations and kinetic experiments. The properties of the SQ are also reproduced quite well, but are mechanistically linked to formation of SQ through reaction 1 above, so that the SQ observed is in the form cyt $b_H H^{\cdot} Q^{\cdot -}$. An interesting feature of these simulations was that, because of the importance of E_m of heme b_H and the Q/SQ couple in Eq. (3), the pH dependence of both b_{150} and the SQ were well explained, but are determined by a single p*K*. Previously we have used the published p*K* at ~7.8 on the heme b_H. However, we have recently revisited these titrations (see below) and now prefer a p*K* in this range on the semiquinone, or associated with interaction with the protein (cf. [69]).

1.3.3. The forward reaction

The mechanism for formation of the cyt b_{150} state provides the main elements of a mechanism for the forward reaction [2]. Additional parameters needed are those for reduction of Q to SQ by electron transfer from heme b_H. The fact that the observed rate is that of the limiting step at the Q_o-site restricts use of the kinetic data to estimation of lower limits for the forward rate constants. However, the equilibrium constant can be estimated from the kinetics with the quinone pool initially oxidized (and the site presumably occupied by Q). After flash activation to populate the ferroheme b_H (generated as the one QH_2 in the pool produced by excitation of the RC is oxidized through the Q_o-site), the heme remains partly reduced in the 100 ms range, suggesting an equilibrium constant for reduction of Q by heme b_HH with $K_{eq} \sim 3$. This relatively stable level of heme b_H reduction titrates away as the pool starts to become reduced over the range below $E_{h,7}$ 150 mV. This is the range over which the cyt b_{150} state is populated, so the acceptor at the site will change from Q to SQ over this range. A mechanism for the forward reaction can then be formulated, as discussed more extensively elsewhere [2].

2. Can a monomeric mechanism account for the observed functional data?

The structures all show a dimer, which raises the main question to be discussed in the remainder of this paper. What do we know of the consequences of this dimeric nature? Are there mechanistic parameters dependent on interactions across the dimer interface?

The structures now available (including several structures from two *Rhodobacter* species [31,32,87]) have demonstrated the high degree of conservation of catalytic subunits across the bacterial/mitochondrial divide, highlighted the dimeric nature of the complex, and provided a framework for extensive discussion of the role of the dimer in mechanism [6,7,53,102–106]. The attractiveness of the modified Q-cycle treatment rests on the fact that the properties can be related to a few constants, measured directly from thermodynamic or kinetic experiments on the intact membrane systems, or calculated from structural data. It is appropriate to emphasize that the kinetic data for native and mutant strains accumulated over the past 25 years have allowed us to subject the modified Q-cycle model to detailed analysis in terms of stoichiometric ratios of reactants, the equilibrium constants determining their distribution, and the kinetic constants determining the time course of changes on introduction of substrates [12,37,107–110]. Because the system can be flash-activated, no mixing of substrates is needed, and as a consequence, the initial state of the

system can be manipulated over a wide range of E_h and pH to change substrate concentrations, thermodynamic poise, etc. These data are satisfactorily and economically explained by the monomeric modified Q-cycle. No *ad hoc* intrusions spoil the simplicity; — there is no need to introduce secondary interactions between sites, or actions-at-a-distance, beyond those introduced by simple coulombic considerations. The mechanism is completely natural, — a conclusion reinforced by more recent data in which kinetic contributions were more accurately resolved by deconvolution, allowing finer points to be explored [111–113]. This is in contrast to schemes introduced by other groups, in which mechanistically occult interactions between catalytic centers, or between reaction intermediates and redox states, have been proposed, which have been given prominent controlling roles [10,53,103,104]. These speculative interactions are based on interpretation of kinetic experiments, usually using an isolated mitochondrial complex in stopped-flow mixing protocol. Although this approach has been applied with skill, intrinsic difficulties limit the utility of some experiments. These arise from the nature of the system, — the experiments require the detergent solubilized complex, and use of more soluble quinol substrates than the native ubihydroquinone-10. As a result, the binding of QH_2 leading to formation of the ES-complex is always unnatural. Even with decylUQH_2 or analogs with truncated isoprenyl sidechains, binding involves partition from a mixed aqueous and micellar phase in which the quinol has a limited aqueous solubility [114] (CMC ~ 30 μM). Often, quinones without the lipophilic side chain, and with very different redox properties (menaquinone or duroquinone, for example) have been used, and these differences change both the kinetics of binding and the equilibrium constants for partial processes, with sometimes dramatic kinetic consequences ([115] and Kokhan, O. and Wraight, C.A. personal communication), so that the observed effects often differ from those seen *in situ*. Because of the limitations of stopped-flow, one has to be careful in interpreting the results, — in particular when using them to justify hypotheses about the physiological mechanism. There is a strong temptation to presume that any kinetic effect that cannot be understood in terms of the simple model must reflect some new twist to the Q-cycle theme, and this has encouraged much speculation centered on "hidden" interactions. Unfortunately, the scope for speculation increases dramatically, with a power-law dependence on the number, *n*, of such interactions proposed, further compounded by a square function if interactions between monomers in the dimer are considered.

We will take as a starting point for discussion the mechanism summarized in Fig. 1, and examine the hypothesis that this minimal model of a monomeric mechanism [2–5] is sufficient to account for the metabolic role of the bc_1 complex. Although the structure is dimeric, the model can accommodate those features from the structural evidence that involve the dimer in a scaffolding role. The iron–sulfur subunit of one monomer is structurally constrained by specific interactions at the membrane level, involving a clamp between cyt *b* subunits, and interactions with other subunits mainly in one monomer, which leave the extrinsic mobile head free to interact with catalytic interfaces in the other monomer. This dimeric involvement could in principle account for the dimeric nature without any extraneous functional role. However, several labs have claimed to demonstrate inter-monomer electron transfer [6,53,103], and others have assumed on the basis of strong theoretical grounds that this must occur [7]. Furthermore, a substantial body of evidence has shown that binding of antimycin modifies the interaction of ISP so as to change the susceptibility to proteolytic cleavage [116], and recent results from Daldal's group have shown conditions in which the g-tensor of the [2Fe–2S] cluster appeared to change with respect to the orientation of chromatophore films on binding of antimycin [102]. Both these latter effects are discussed in the context of a modified interaction with the Q_o-site occupant, reflecting a coupled conformational change induced by antimycin binding at the Q_i-site.

As several commentaries have noted [7,27,53,117], the structures show distances between the b_L hemes across the dimer interface that are expected to facilitate rapid electron transfer. These are Fe–Fe at 21.58 Å, nearest conjugate atoms at 10.54 Å (vinyl sidechains), and pyrrole rings at 14.45 Å (in 1pp9) (Fig. 3A). Values for rate constant depend on which distances is used, and on whether a classical Marcus [118,119] or Moser–Dutton [120–124] treatment is used for the exponential term. Some representative values for the competing pathways are shown in Table 2. If the appropriate distance is that between conjugate systems, it would likely include the vinyl sidechains, the path assumed in the Table. The values for ΔG chosen depend on the redox status, and hence on any effect of coulombic interactions between hemes. For example, if heme b_H is reduced in one monomer, the coulombic effect on b_L will be about −60 to −80 mV, generating an exergonic pathway for electron transfer to the neighboring heme b_L, if the heme b_H in that monomer is oxidized (bottom line). Note however that all b_L–b_L rate constants would allow rates more rapid than the rate-determining step ($\sim 1.35\times10^3$ s^{-1}) [25,26]. A succinct review of this problem by Shinkarev and Wraight [125] is couched in terms of competition between the heme b_L→ heme b_H, and heme b_{L1} → heme b_{L2} paths. In assigning rate constants, they assumed the appropriate distance was that between conjugate rings, (14.45 Å), but since the vinyl groups are part of the conjugate system, it does not seem natural to exclude them, and this increases rate constants by a factor of ~200. Then, although competitive effects could lower expected rates as they suggest, under conditions in which both hemes b_H are oxidized, no combination of effects within the conventions of the Moser–Dutton treatment of the intrinsic rate constant would prevent electron transfer across the dimer interface at rates in the range of the limiting rate once the "active side" b_H became reduced. The expectation is therefore that electrons could be shared between monomers at this level, and that this pathway would be functional, and easily observable on the time scale of ~100 ms used in typical experiments.

Experimental evidence in support of dimeric operation has come from several studies. Covian et al. [126] interpreted stopped-flow kinetic experiments as showing that the stoichiometry of cyt c_1 reduction on addition of decylUQH_2 was half that expected from the total complement, and that only half of the complex present participated in electron transfer. Under these conditions, two cyt *b*-hemes became reduced per active enzyme in the presence of antimycin (although no effort was made to distinguish between hemes b_H and b_L). These properties were similar to previously observed kinetic anomalies, which were explained by the modified Q-cycle. For example, on flash activation in the presence of antimycin, a discrepancy between amplitudes of heme b and heme c reduction is observed, and had been seen as contrary to the expectations of a Q-cycle [127]. However, the modified Q-cycle requires two turnovers of the Q_o-site for a full turnover of the complex, and detailed analysis in the early 1980s showed the equilibrium constant for these depends on the acceptor. The value depends on E_m for heme b_H on the first turnover (K_{eq} ~ 480), and that of b_L on the second turnover (K_{eq} ~ 3), and the degree of reduction of the high-potential chain is simply a reflection of this change in the nature of the acceptor [12]. However, Covian et al. [126] explained their results in terms of an anti-cooperative mechanism in which the Q_o-site of only one monomer was functional, but fed into both sides of the dimer through electron exchange at the heme b_L level. In support of this, they showed titration curves with antimycin of the initial rate of cyt *c* reduction in a steady-state assay of activity that gave a convex curve, with a stimulation of rate in the sub-stoichiometric range. In a later paper [6], the same group reported titrations by antimycin of cyt *b* reduction on addition of decylUQH_2 to the myxothiazol inhibited complex, in which the titration curves showed a convex shape. They again interpreted the results as showing electron transfer between the b_L hemes.

Although such convex curves might be expected from electron-sharing, a substantial literature from the 1970s, following the observation of Kröger and Klingenberg [128,129] of hyperbolic titration curves

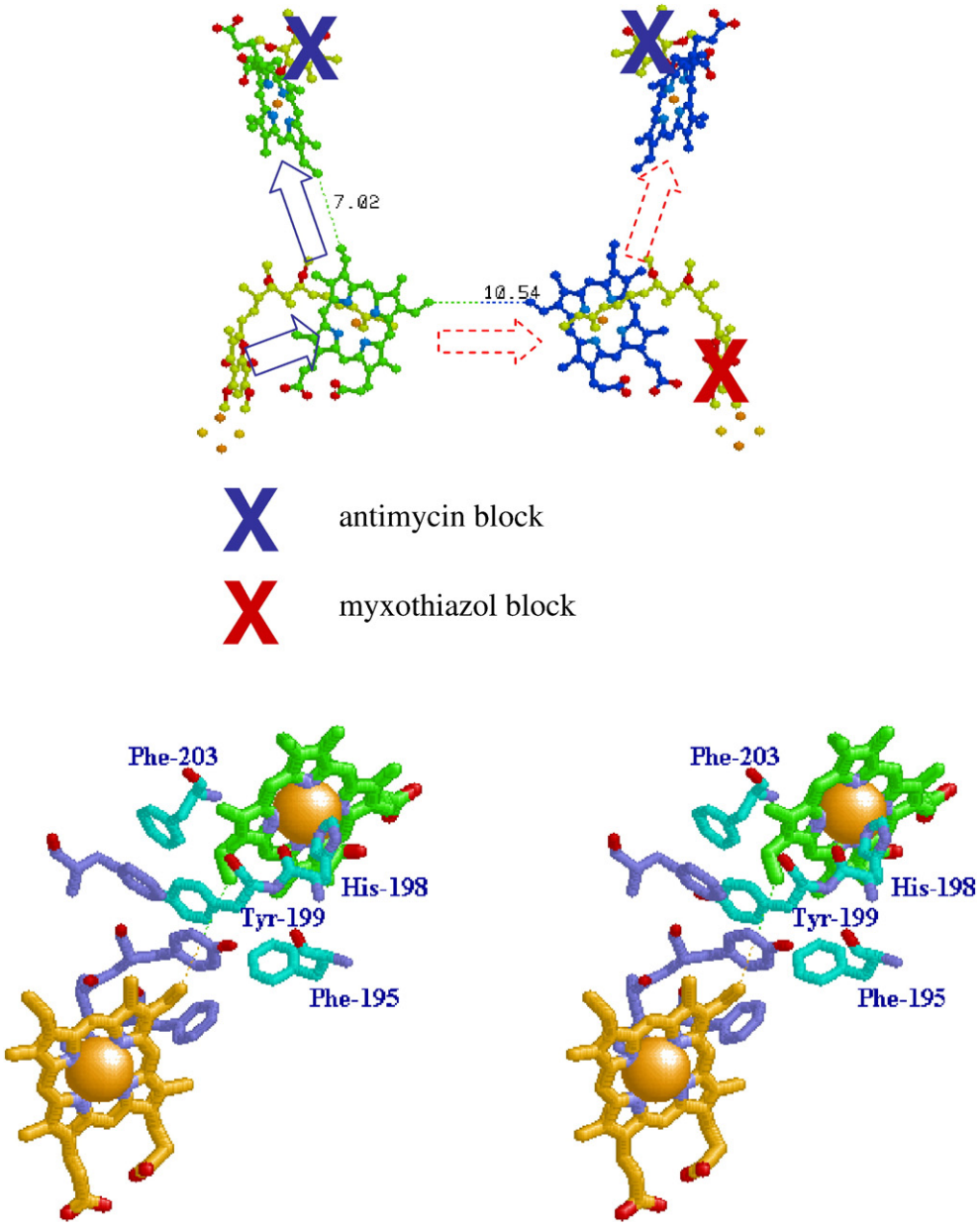

Fig. 3. Schemes to show potential electron transfer pathways involved in electron equilibration between monomers at the level of heme b_L. Top. The redox centers of the dimer are shown, and the Q_o- and Q_i-sites indicated by stigmatellin and antimycin, respectively. The scheme shows the dimer with the Q_i-site blocked in both monomers by antimycin (blue crosses), and the Q_o-site of one monomer blocked by myxothiazol (red cross). Under these conditions, if electron transfer between hemes b_L could occur, both hemes b_H could be reduced by turnover of the uninhibited Q_o-site (broken red arrows). Bottom. The dimer interface, showing residues referred to in the text. The dotted line shows the 10.21 Å distance between heme b_L 4-vinyl groups (taken from PDB file 2qjy, chains A–F).

with antimycin resulting from a "pool" effect of ubiquinone, demonstrates that alternative explanations are possible. In general, a Kröger–Klingenberg effect will be found whenever the turnover of the process being titrated is greater than that of the rate-limiting reaction, since a fraction of centers can be eliminated without a full effect on the overall process. We have been able to generate convex titration curves under a variety of such conditions with chromatophores ([130], and in collaboration with Vlad Shinkarev), or with isolated bc_1 complex. However, when care was taken to ensure that the rate-limiting step was the process titrated, linear curves were always seen. Indeed, such linear titrations are the norm in the literature. Several other mechanisms can give non-linear titration curves, as shown on titration of the amplitude of cyt c_1+c_2 oxidation following flash activation in chromatophores [130], where the degree of convexity is dependent on which time-point in the kinetic curve is chosen. This is because mobility of the substrates QH_2 and cyt c_2 allows one active complex per chromatophore to re-reduce all cyt c_2, given time. This effect has an n-value from Hill plots of ~9, likely reflecting the number of bc_1 complexes per chromatophore. Similarly, titration by antimycin of the kinetics of cyt b_H reduction and

Table 2

Reaction pairs and conditions	Moser–Dutton k/s^{-1}	Marcus k/s^{-1}
b_L–b_H 2-vinyl (assuming ΔG=−60 mV, λ = 0 .75, R=7.02 Å)	8.97×10^8	1.73×10^8
b_L–b_H 2-vinyl (assuming ΔG=−130 mV, λ = 0 .75, R=7.02 Å)	2.15×10^9	5.68×10^8
b_L–b_L 4-vinyl (assuming ΔG=−0 mV, λ = 0 .75, R=10.54 Å)	2.86×10^6	4.08×10^5
b_L–b_L 4-vinyl (assuming ΔG=−60 mV, λ = 0 .75, R=10.54 Å)	6.51×10^6	1.25×10^6

re-oxidation shows a similar effect, possibly, as suggested by Bechmann et al. [131], because antimycin can leave one Q_i-site and find another, so long as one remains open. In the isolated complex this gave an *n*-value of 2, but we found a higher value in chromatophores (>4.9) (Fernandez-Velasco and Crofts, unpublished), which suggests that the inhibitor can redistribute as long as an open site is available in a chromatophore. In

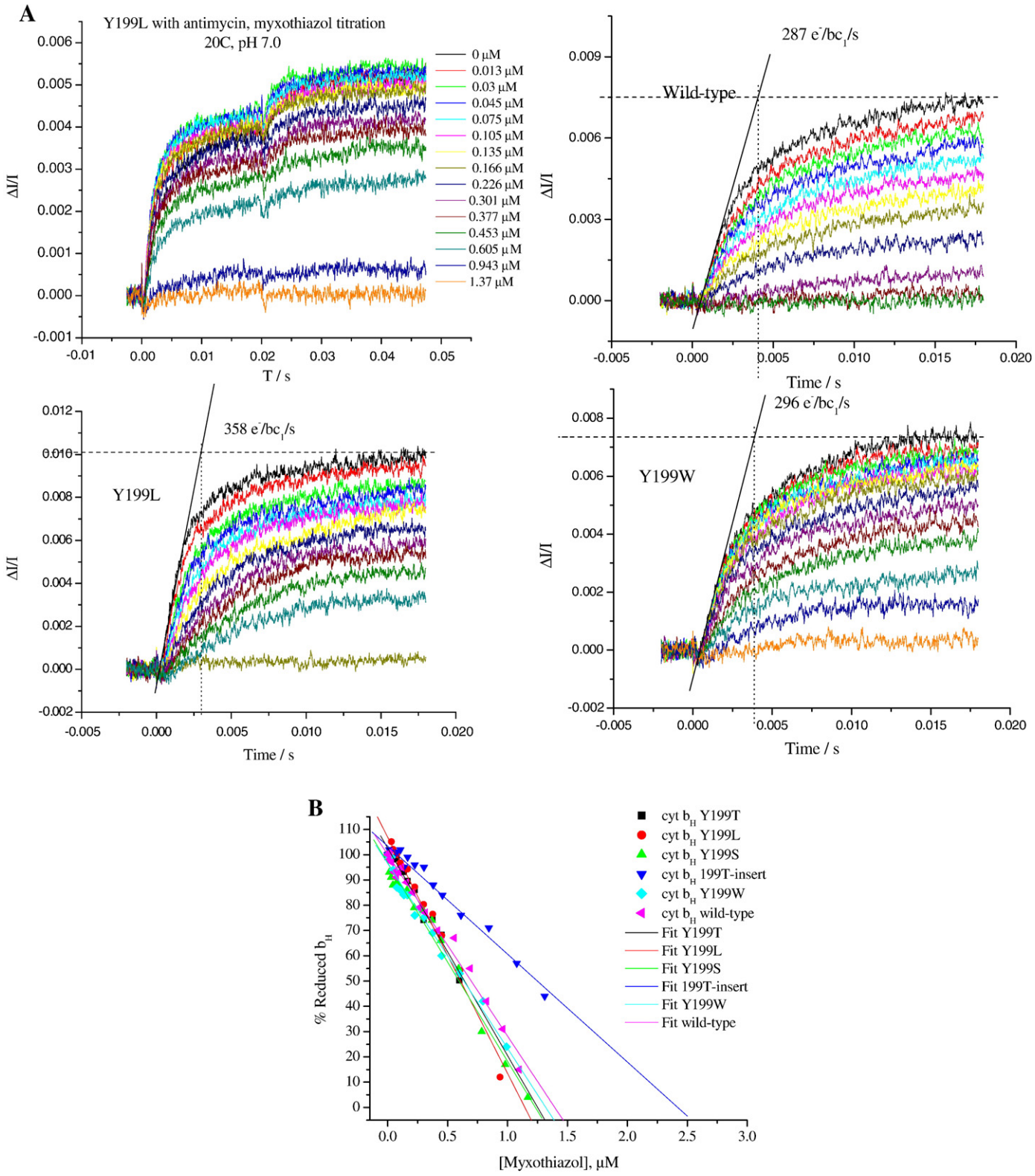

Fig. 4. Titrations of Q_o-site with myxothiazol showing linear curves in WT and mutant strains. A) Typical curves showing the kinetics of heme b_H reduction in WT in the presence of antimycin. Similar sets of data were taken for each strain, all of which had similar maximal rates. Myxothiazol concentrations are indicated to the right of each curve. B) Fraction of heme b_H reduced at 20 ms (expressed as %) in the presence of Q_i-site inhibitor antimycin A, as a function of inhibitor concentration. The system was excited with a xenon flash (~5 µs at half-height) and the reduction of b_H monitored from the difference kinetics measured at 561–569 nm. Ambient redox potential was poised at ~100 mV (QH_2 oxidation close to maximal). Strains are indicated by labels; bc_1 complex in the range 70–220 nM.

both cases, linear titrations are seen under conditions in which the rate-limiting step was titrated.

$$K_{eq} = \frac{k_f}{k_b} = \frac{\left[b_L^-\right]^2}{\left[b_H^-\right]^2} = 10^{\Delta E_m/(59.19)} = 0.054 \quad (4)$$

$$K_{eq} = \frac{k_f}{k_b} = \frac{\left[b_H b_L^-\right]}{\left[b_H^- b_L\right]} = 10^{\Delta E_m/59.19} = 0.0029 \quad (5)$$

In the work from Covian and et al., the case for an interpretation in terms of electron exchange between monomers depended on a kinetic model in which a questionable value for the equilibrium constant between hemes b_H and b_L was used [6,126]. The treatment involved a reaction equation, $b_H^- + b_L \leftrightarrows b_H + b_L^-$, appropriate for the reaction in the solution. Then a condition $[b_H^-]=[b_L]$, and $[b_H]=[b_L^-]$ was imposed because the actual reaction was intramolecular (Eq. (4)), and this changed the equilibrium constant determining occupancy of the b_L^- state by 18.6-fold (compare Eqs. (4) and (5)). The value derived allowed sufficient occupancy of the b_L^- state to provide an inter-monomer rate that explained the observed rate. Without the larger value for K_{eq} their model fails to match the kinetic data. The treatment is in error on both mechanistic and thermodynamic counts; the reaction is not 2nd order, and by assigning separate identities to four reactants, they are trying to have their entropic cake and eat it too. Intramolecular electron transfer is an exchange between two states in which the electron is on either the one or the other center, and treating the system as 1st order gives the conventional equilibrium constant expected from a one-electron transfer. For the transition $b_H^- b_L \leftrightarrows b_H b_L^-$, K_{eq} is determined as in Eq. (5). Any alternative path with a different equilibrium constant would make possible a perpetual motion machine. Because the experiments of Covian et al. [6,104,126] did not discriminate between several possible mechanisms, and because their model is suspect, it can hardly be taken as established from these results that the mechanism is dimeric, or that electron exchange must occur between monomers on the time scale of turnover.

Gong et al. [104] have constructed mutants in *Rb. sphaeroides* with changes at three aromatic residues, Phe-195, Tyr-199, and Phe-203, which, on the basis of a computer model, were expected to line the dimer interface between the b_L hemes. They studied steady-state electron transfer and SO production in bc_1 complex isolated from variants in which each residue was changed to alanine, with some additional changes at F195. The electron transfer rates reported (2.5 μmol cyt *c* reduced/nmol heme *b*/min or 21 mol/mol/s for the wild-type) were only ~1.5% physiological rates (1350 mol/mol/s at saturating substrate), indicating that the turnover was substantially inhibited in all these preparations. None of these mutations had a strong inhibitory effect. The greatest effect was seen when Phe-195 was changed; F195A had a lower rate (80% of WT) than F195W, F195H or F195Y, and a higher rate of SO production. On this basis, the authors concluded that an aromatic residue was required, and that the critical function was the electron transfer between the b_L hemes. However, this electron transfer path was conjectural; no evidence was presented showing that any such reaction occurred, and the effects could as well have been attributed to a weak inhibition of the Q_o-site, which (on the basis of myxothiazol occupancy) is 14–19 Å from these residues. In structures now available, only Tyr-199 is in the most direct path, whether interpreted as through bond or through protein. We discuss below our own results based on a series of mutations at this residue, Y199T, S, C, W and L, and show that these are clearly against an inter-monomer exchange.

In another challenge to the modified Q-cycle, Mulkidjanian [9,10] has suggested an "activated" Q-cycle with a number of novel features, at least some of which seem untenable. He attributed the acceleration of the rate of QH_2 oxidation in the range ~E_h 150 mV to a priming process involving formation of SQ at the Q_i-site (the cyt b_{150} effect). However, the same acceleration over this E_h range occurs in the presence or absence of antimycin, which specifically eliminates the Q_i-site SQ, so this must be wrong. It had previously been demonstrated that this acceleration was due to an increase in $[QH_2]$ on reduction of the Q-pool, and preferential binding of QH_2 at the Q_o-site [12]. Another odd experimental result under special conditions was a marked difference in rates of turnover of the Q_o-site in the presence or absence of antimycin. However, this contradicts studies from a number of labs [12,37,132–135]] showing the rates to be the same under these two conditions. It seems likely that these aberrant observations reflect a lack of technical finesse rather than real functional differences.

Other groups have suggested control functions based on conformational coupling linked to structural changes on occupation of the Q_o-site by different redox species [39]. However, the causal relationship proposed could be as well explained by dynamic flexibility to accommodate different reaction partners [40].

3. Myxothiazol titrations to test for electron transfer between monomers

In the presence of antimycin, oxidation of heme b_H is prevented, so electrons passing out of the Q_o-site accumulate in heme b_H. In chromatophores, the stoichiometry of reaction centers to bc_1 complex is about 2:1, ensuring that sufficient substrates (2 cyt c_2^+ plus $1QH_2$) are generated on a saturating flash to allow one full turnover of the complex. In the presence of antimycin, the two oxidizing equivalents in the high-potential chain could in principle oxidize 2 QH_2, with reduction of hemes b_H and b_L. However, the equilibrium constant for the second turnover, resulting from the low E_m (~−90 mV) of heme b_L, prevents this, restricting the complex to 1 turnover of the Q_o-site [24,109]. If inter-monomer transfer could occur [27,53,104,117], electrons from either Q_o-site in the dimer could reduce both hemes b_H. Even with one monomer per dimer inhibited at the Q_o-site by myxothiazol, full reduction of heme b_H should be observed, because both b_H centers would operate at the same higher E_m (~40 mV), so that the equilibrium constant would strongly favor reduction. In practice, statistical effects would lead to a bowed titration curve (for example, at 50% occupancy, the distribution of dimers expected is 25% each of 0,0; 0,1; 1,0; and 1,1, where 0 and 1 are vacant and myxothiazol inhibited sites, so 75% of the full reduction might be expected). This convex titration curve is not seen. This could possibly be attributed to some special role for the intervening protein. We have constructed mutant strains in which the residue at the contact point between monomers at the level of heme b_L, Tyr-199, was modified to give Y199 W, T, S, L, and C. Since this residue is next to His-298, a ligand to heme b_L, and lies on the most direct path of electron transfer between hemes b_L (Fig. 3B), we anticipated substantial effects when inter-monomer electron transfer was probed by titration with myxothiazol (Fig. 4). Fig. 4 shows the results observed. All strains showed similar rates for Q_o-site turnover in the absence of myxothiazol. None showed any marked change in redox properties of the cytochromes (Table 3), although all showed small changes in the α-band spectrum of heme b_L. Titrations for all strains (including WT) were strictly linear, whether measured through initial rate, or amplitude of reduction, or

Table 3

Strain	Redox potentiometry E_m, (V)			Nernst equation solution fitted at each wavelength of the spectrum, E_m, (V)				
	b_L	b_H	b_{150}	Cyt c_1	b_L	b_H	b_{150}	Cyt c_1
WT+antimycin	−0.113	0.049	–	0.250	−0.090	0.040	–	0.250
WT	−0.120	0.054	0.169	0.250	−0.090	0.040	0.150	0.250
Y199L	−0.123	0.038	0.149	0.259	−0.100	0.030	0.148	0.250
Y199S	−0.077	0.057	0.172	0.265	−0.094	0.053	0.170	0.260
Y199T	−0.108	0.045	0.160	0.262	−0.092	0.027	0.152	0.250
199-insert	−0.096	0.035	0.155	0.251	−0.092	0.033	0.135	0.250
Y199W	−0.080	0.075	0.170	0.237	−0.091	0.050	0.150	0.250

after 1 flash or two (Fig. 4B). Since the second flash leads to re-oxidation of the high-potential chain, the driving force for inter-monomer electron transfer would be substantially increased, and an "extra" reduction of heme b_H would have been expected if electron transfer between the b_L hemes could occur, but this was not observed. Instead, heme b_L went reduced after the second flash, as expected in the monomeric Q-cycle [12]. Furthermore, no indication of the biphasic character expected from a branched pathway was apparent in the kinetic curves. We also tested these properties in a strain (H198-T199-Y200) constructed so as to mimic the extra residue in the sequence at this point found in the cytochrome b_6f complex of the cyanobacterial/chloroplast photosynthetic chain (with sequence -HTF-) [136]. Again, myxothiazol titrations were linear, although the structures now available show a distinctive change in configuration of the interface in the b_6f complex compared to the bc_1 complex, which might also have been induced by the mutation. The simplest interpretation of these results is that no inter-monomer electron transfer occurred, despite the short distance between the hemes and the rapid rate constant expected.

The above conclusion presents an interesting paradox. From treatments using the Moser–Dutton approximation for intrinsic rate constant at this distance, electron transfer should occur, but the experiments show that it does not. If unequivocal evidence becomes available showing that

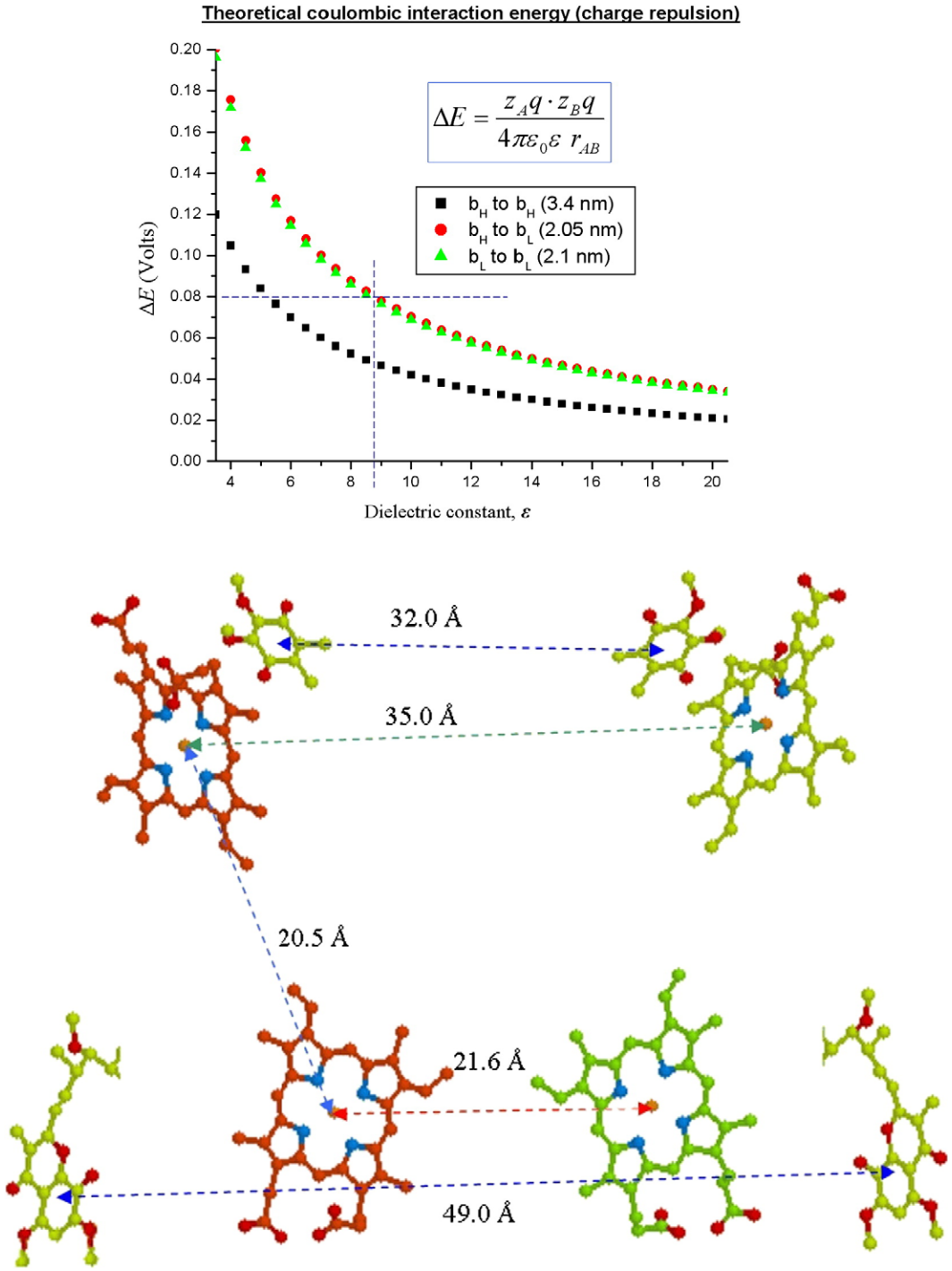

Fig. 5. Coulombic free-energy change expected between hemes. The change in E_m expected from coulombic effects between hemes calculated from distance apart, for different intervening dielectric values.

electron-sharing occurs, then the data interpreted as showing that it does not will have to be re-evaluated. If on the other hand, no such evidence is found, then it will be necessary to explore the possibility that other parameters must be important in determining electron transfer rate, over and above those in the Moser–Dutton treatment. Either result would be of interest, and advance the field.

Several possibilities look interesting. The Moser–Dutton treatment uses the Hopfield approximation [119] to allow for quantum mechanical effects, but this effectively modifies k_B, giving rise to thermodynamic inconsistency in applying the Marcus term to the Arrhenius expression [137]. From the Marcus curve generated using Moser–Dutton value of 3.1, values for $\log_{10}k$ at any chosen ΔG appropriate for a forward reaction, and for a reverse reaction at a value taken symmetrically with respect to $\Delta G=0$, do not give the ratio expected from the relation of ΔG to K_{eq}. In the Moser–Dutton treatment of the intrinsic rate constant, the approach is implicitly classical, since fluxes through all pathways are additive, and distance and density are taken to provide all information pertinent to the probability of electron transfer through the protein matrix. Alternative approaches have treated the intrinsic rate constant quantum mechanically [119,138]; then a standard path integral treatment opens the possibility of destructive interference, so that, in this scenario, interference in the inter-heme b_L path could limit rate. Indeed, several recent papers [139–143] have considered more sophisticated treatments that include interference terms. In a few cases, especially those involving pathways including heme and the liganding histidine, destructive interference was found to play an important role. Additional complications arise in systems involving electron transfer between subunits [142]. A more conventional approach is in terms of the electron distribution on the hemes. If the electron distribution at the 2-vinyl position is more favorable than at the 4-vinyl, this would favor electron transfer from heme b_L to b_H. Walker [144,145] has kindly provided useful insights into the electronic structure as determined by calculation and EPR, and has provided data showing that the β-carbons of the 2-vinyls of the ferrihemes should both have substantially higher spin occupancies than those of the 4-vinyls (Ann Walker, personal communication). Since rate depends on k[occupancy], the $b_L \rightarrow b_H$ pathway (in which the 2-vinyls are in the shortest path) should be favored.

4. Coulombic interactions in the dimer

When the bc_1 complex was mutated to replace one of the histidine ligands to heme b_H, the complex was still assembled with a full

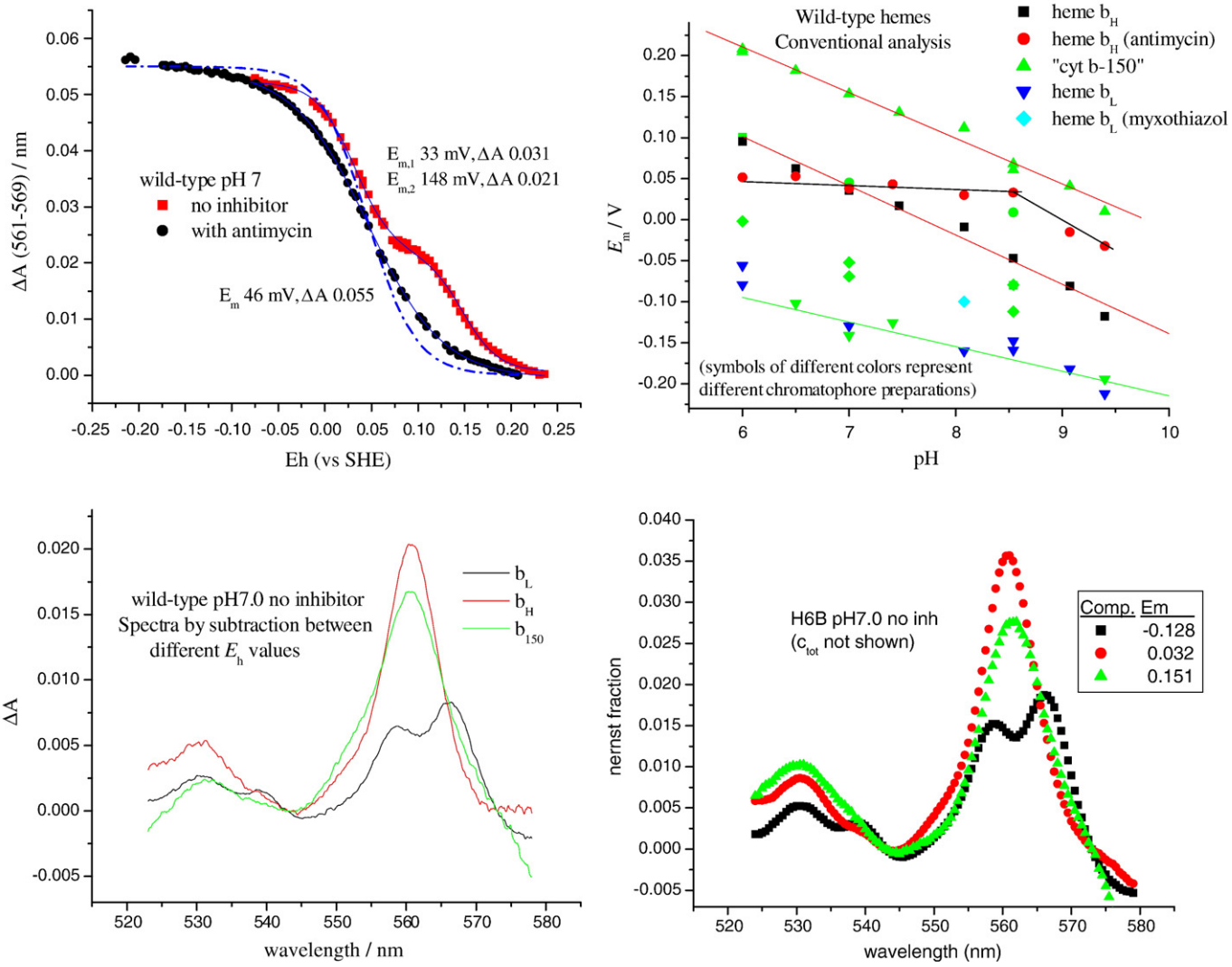

Fig. 6. Thermodynamic behavior of the *b*-type hemes in H6B strain (his-tagged cyt *b* with wild-type sequence) *in situ*. (Top left) typical titration data in the absence and presence of antimycin (pH 7); (bottom left) spectra from redox cuts showing cyt b_{150}, heme b_H and heme b_L; the dashed line shows the curve expected for an $n=1$ component, with amplitude for degree of reduction plotted as $\Delta A = 0.055\frac{1}{10^{(E_h-E_m)/59}+1}$. (Bottom, right) spectra derived by fitting titrations at each wavelength using fixed values for E_m, and n, for each component; (top, right) the pH dependence of E_m values for individual components, assuming single species for each component.

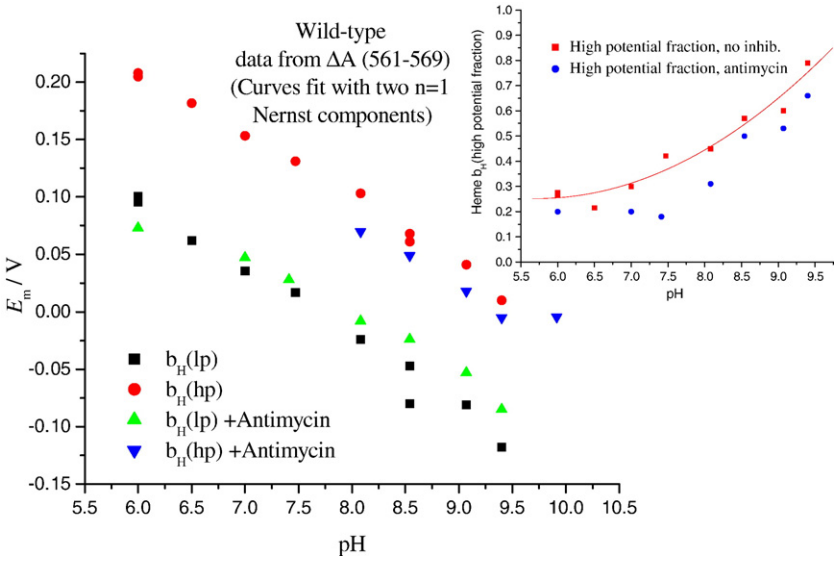

Fig. 7. Reanalysis of the thermodynamic behavior assuming the coulombic effects are in play. Titration data for heme b_H in the absence or presence of antimycin were assumed to reflect two components split by coulombic interaction.

complement of redox centers, except for that heme. The complex retained a fully functional Q_o-site reaction, but turnover was restricted by the availability of heme b_L as the only low-potential chain acceptor [146]. Potentiometric titration of the hemes showed that the $E_{m,7}$ values for heme b_L were changed from ~−90 mV in wild-type to −8 mV (in H111N) or −14 mV (in H212D), an increase of ~80 mV. We suggested that this change could be explained by loss of a coulombic interaction on the loss of the negative charge of heme b_H, which, with E_m ~ 50 mV, would be reduced over the range in which heme b_L titrates. If this speculation is accepted, the value and the distances shown by structures would allow calibration of other coulombic interactions in the dimeric complex, and construction of the curves like those shown in Fig. 5. From this, it is evident that substantial coulombic effects might be expected both within the monomer, and across the dimer interface. Such interactions have been extensively investigated in other systems. In order to explore these possibilities, we have re-evaluated the thermodynamic properties of the *b*-hemes by analysis assuming such effects.

4.1. Thermodynamic properties of the b-hemes

Titrations were performed using full spectral analysis over the α- and β-band range, long equilibration times between measurements, and relatively high concentrations of mediators. Typical curves are shown in Figs. 6 (wild-type) and 8 (mutant N221I) [147]. Space does not permit a full discussion, but several interesting features emerge from this new analysis.

i) The p*K* at 7.8 previously observed is not seen [91,92]. It seems likely that in previous analysis, titration curves for heme b_H were convoluted with cyt b_{150} and the pH dependence of its amplitude (Fig. 6). Two brief reports suggest that the same is true in *Rb. capsulatus* [7,66].
ii) A second new observation is the apparent independence of pH for the E_m values for heme b_H in the presence of antimycin.
iii) Finally, in fitting the curves, especially those for b_H in the presence of antimycin, and for b_L, we found that *n*-values less than 1 often provided better fits (Fig. 6, top left). When $n=1$ was imposed, analysis of the curves into two components was required for a good fit (Fig. 7).

Because small changes in the extremes of the fitted curves can give quite large differences in fitted values, the data presently available are not accurate enough in themselves to provide unambiguous values. Furthermore, analysis was complicated by the presence of additional components from other redox complexes, most notably a heme with a spectrum similar to heme b_H titrating in the range of the cyt b_{150} component, which was not observed in titrations of the isolated complex, but which contributed 10–15% of the measured change in chromatophores. With these necessary caveats, when an analysis of

Table 4
Kinetic characteristics of strains with Asn-221 of cytochrome *b* modified

Strain	Photosynthetic growth	Reduction of b_H[a]	Fraction of b_H reduced[b]	$E_{m,7}$, pH dependence[d]			Re-oxidation ($t_{1/2}$/ms)[e]
				Cyt b_{150}	b_H, no inhibitor	With AA	
Wild-type	+++	455	0.05	148, −59	32, −59	46, 0	<1.6
N221D	+++	(as wt)	0.8	150, −59	35, −54	−47, −59	15
N221H	+++	520	0.68	150, −59	35, −59	13, −50	12
N221P	+++	442	0.167	154, −59	38, −59	−3, −59	2.0
N221T	+++	(as wt)	0.37	140, −59	29, −50	13, 59	8.0
N221I	+++	(as wt)	0.75	104, −59	36, −59	−95, −59	14

[a]Rate of reduction of heme b_H measured following a 5 μs flash at E_h ~ 120 mV in the presence of antimycin (units — mol cyt b_H/mol bc_1 complex/s).
[b]Fraction of heme b_H reduced at the maximal amplitude (at ~3–5 ms) of the kinetic trace in the absence of antimycin, compared to the fraction reduced in the presence of antimycin.
[c]Rate of re-oxidation of heme b_H in the absence of antimycin, measured by subtraction of the traces in the presence and absence of antimycin (units — mol cyt b_H/mol bc_1 complex/s). The rate in the wild-type reflects the rate-limiting reduction of the low-potential chain through the Q_o-site reaction. Since $v=k$(occupancy), and the fraction of heme b_H in the reduced form (column 4) is <<1, the rate constant must be much greater than that for the limiting step.
[d]$E_{m,7}$ in mV, pH dependence of E_m in mV/pH unit, assuming a single component for each heme.
[e]Half-times for re-oxidation of heme b_H measured from kinetic traces.

heme b_H was performed, assuming that each component of the bc_1 complex was split, some additional features became apparent (Fig. 7). The titration was resolved into two components in the presence or absence of antimycin, each showing the same pH dependence. The lack of pH dependence for heme b_H in the presence of antimycin disappeared, and was seen to reflect a pH dependence of the amplitude of a higher-potential component. The higher-potential component in the presence of antimycin had a lower E_m than the cyt b_{150} component, and so was merged with the low E_m component to give what appeared to be a single component. We hesitate to put too much emphasis on this reanalysis, but it suggests two populations with the same spectrum titrating with different E_m values, which is the behavior expected from two hemes in identical environments interacting through coulombic repulsion. Clearly, a more detailed analysis with full electrostatic calculations (cf. [69]) is needed, since the local fields and dielectric properties are not well represented by mean values assumed in Fig. 5.

4.2. Asn-221 mutants

Similar experiments with strains N221T, H, I, S, P and D have shown dramatic effects on the thermodynamic parameters measured in the presence of antimycin. Effects of mutation are also reflected in major changes in kinetics. These experiments are still in progress, but example data have been reported elsewhere [90,147], and are summarized in Table 4.

Several interesting effects can be noted in these data. In all Asn-221 mutant strains, the redox properties of both *b*-hemes (and the cyt b_{150} component) were relatively unaffected in the absence of antimycin, but E_m values for heme b_H were shifted to lower values in the presence of antimycin, quite dramatically in some strains. However, in the presence of antimycin, the electron transfer rates to the b_H heme were not markedly changed, indicating that turnover of the Q_o-site was unaffected. All mutations showed some inhibition of electron transfer from heme b_H to the acceptor at the Q_i-site in the absence of antimycin. Inhibition was apparent both at $E_h \sim 200$ mV, where the acceptor would be Q, and 100 mV, where SQ is likely the acceptor in WT. Titrations of SQ have shown similar values to wild-type for amplitude and peak of the bell-shaped titration curve in strains so far tested (N221P and S), so we have no reason to believe that the SQ stability is markedly changed. For several strains, rates were substantially slower than wild-type. Surprisingly, N221P, in which H-bonding potential is lost, showed the least kinetic effect.

In the presence of antimycin, all strains showed changes in thermodynamic properties of heme b_H (but not b_L). When analyzed according to conventional single component titrations, all mutants showed a dependence of ~−59 mV/pH. For several strains, the changes in E_m in the presence of antimycin were quite dramatic, as seen in N221I (Fig. 8). This can be seen most easily through the difference spectra in Fig. 8C. In the absence of antimycin, the difference ΔA for the redox cut between $E_{h,8.7}$ values −380 and −40 mV shows a spectrum of heme b_L similar to that over the same range in wild-type. On addition of antimycin, an additional component appears in this difference spectrum, shown as the antimycin induced change, which has the spectrum of heme b_H, but with an E_m shifted to the same range as heme b_L. As with wild-type, the titration data in the mutant strains were not well fit by single components of $n=1$ (Fig. 8B), and this was also obvious in titrations of heme b_L (not shown). Because in some mutants, the two hemes showed similar E_m values, unambiguous resolution of the different components was difficult. The effects of the lowered E_m were apparent in kinetic data, so that in the presence of antimycin at ambient potentials at which the quinone pool was oxidized enough to sustain turnover ($E_{h,7}>40$ mV), and where both hemes were expected to be substantially oxidized, reduction of components with both spectra was observed on flash activation. This is in contrast to wild-type, where reduction of heme b_L was observed only when heme b_H had been pre-reduced before the flash [109]. The interpretation of these results is again ambiguous, but we favor a picture in which coulombic interactions can occur both within the monomer, and across the dimer interface, as shown schematically in Fig. 9.

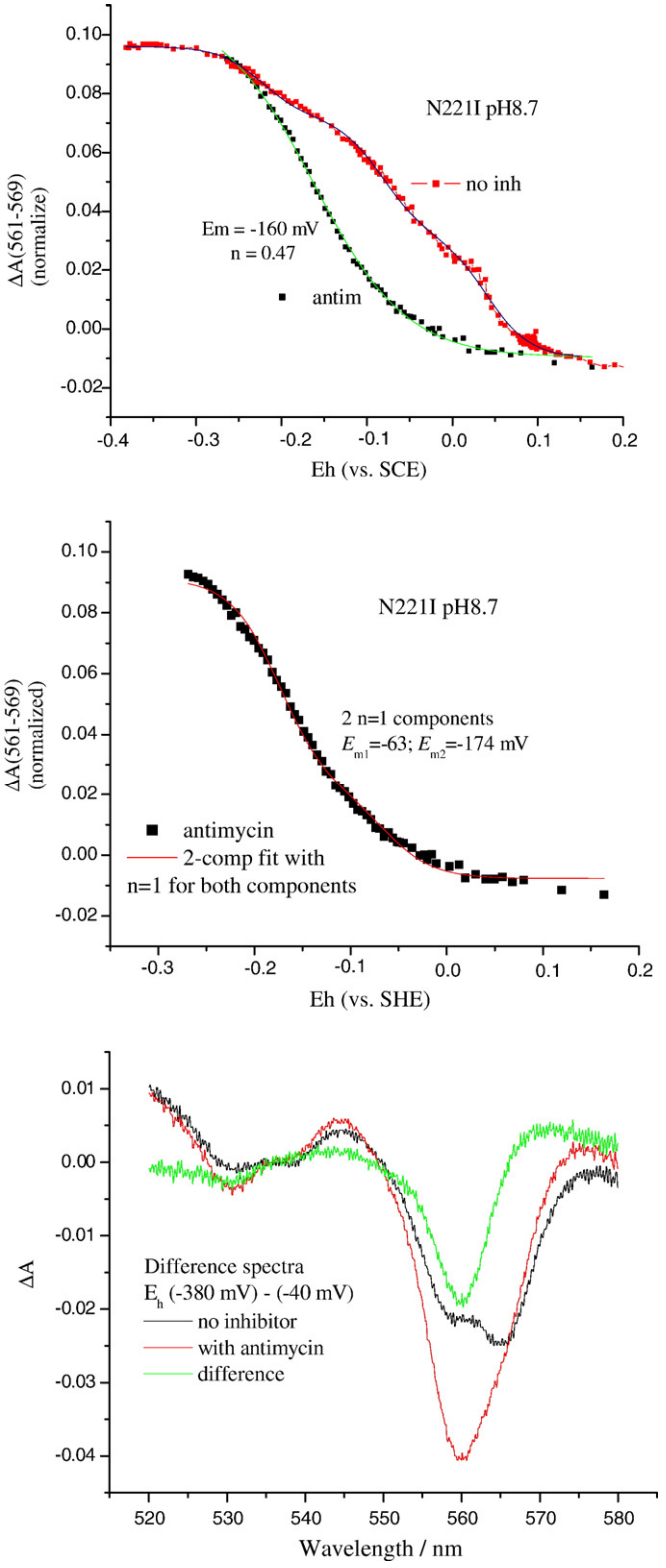

Fig. 8. Titration of heme b_H in chromatophores from N221I in the presence and absence of antimycin. A (top), titration curves showing shift in E_m on addition of antimycin; B (middle), titration with antimycin fit by 2-component, $n=1$; C (bottom), absorbance spectra showing the difference (−380)–(−40) mV from pH 8.7 titration. The difference with and without antimycin shows the contribution of heme b_H with its low potential in the presence of antimycin.

It will be obvious that detailed characterization of these strains, especially with respect to the SQ properties, will provide parameters suitable for testing the hypothesis proposed for cyt b_{150} formation. The dramatic effects of antimycin in the heme b_H properties will also help in understanding how binding can modify these parameters. A comprehensive review of structural aspects of antimycin binding by Huang et al.[86], the electrostatic calculations for the yeast complex [69], and the recent higher resolution structures of the *Rb. sphaeroides* complex [87] have provided a firm basis for discussion. Since the N221P strain showed minimal effects on function in the absence of antimycin, it is clear that the H-bonding possibilities of the asparagine in wild-type are not essential to function [90]. Despite the minimal effect of mutation on function, on addition of antimycin this strain showed a marked shift in E_m for heme b_H. The pattern of this effect among the neutral residue changes tested was for a larger shift in E_m with increasing hydrophobicity. The N221D mutant falls outside this pattern, but this may reflect its acidic nature. There is no obvious feature of these characteristics that allows us at present to suggest a mechanistic explanation. Examination of the protein environment with respect to heme b_H shows a highly polar region, likely related to

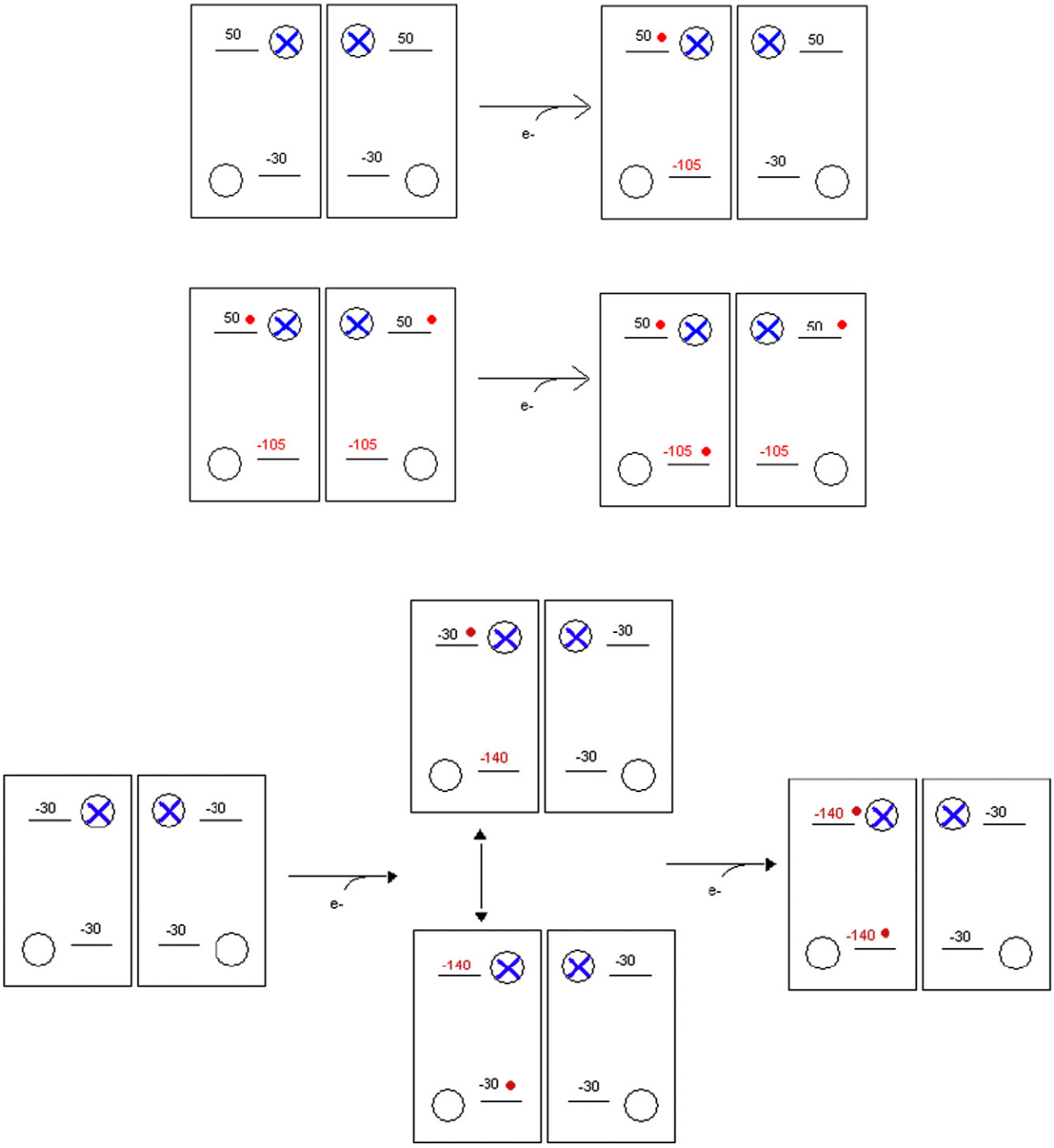

Fig. 9. Scheme to show some of the coulombic interactions suggested. The dimer is represented by four Q-sites (circles) with antimycin blocking Q_i (blue cross). The hemes are shown as horizontal bars, either empty, or occupied by an electron (red dot). Top, in wild-type, heme b_H has $E_{m,7}$ ~ 50 mV, heme b_L has in intrinsic $E_{m,7}$ ~ −30 mV, but titrates with E_m ~ −100 mV because of coulombic interaction with heme b_H. Bottom, in N221I, both hemes have the same intrinsic $E_{m,7}$ ~ −30. The first electron can go to either, and change the E_m of the other. For clarity only the coulombic interactions within a monomer are shown However, the titrations suggest that additional interactions across the dimer interface may also occur.

the need for equilibration of the heme with external pH. If such equilibration were through protonation of the D-propionate of heme b_H on redox change, this volume would be expected to support proton equilibration through H^+ conducting pathways. We have noted previously the extensive H-bonding in this volume, and the presence of a bound water that forms a H-bonding link between the propionate and *Ser-203* in the bovine structure. Since there is considerable variability in conformation within this volume in the six different monomers of the *Rb. sphaeroides* bc_1 complex that are included in PDB file 2qjy, it seems likely that this part of the protein is structurally plastic. It may be involved in equilibration of the heme propionate with the N-phase pH. However, this propionate was not included in the set of residues shown to undergo protonation change in response to reduction in electrostatic studies [69].

In summary, it seems likely that coulombic interactions are "felt" between all centers in the dimeric structure that carry charge. The mechanistic consequences for interactions within a monomer are subsumed under the monomeric Q-cycle, since the E_m values derived from redox titration are those that reflect the interactions. As noted elsewhere, coulombic interactions within the Q_o-site provide a possible mechanism for prevention of bypass reactions [5]. Interactions across the dimer interface have not been analyzed in detail. However, it seems reasonable to look to an interaction between $Q^{\cdot-}$ species in the Q_i-site as a possible explanation for the otherwise anomalous observation that the maximal SQ population observed is a 1/dimer.

5. Conclusions

The modified Q-cycle continues to provide the most economical model for the mechanism of the bc_1 complex. The evidence for inter-monomer electron traffic does not seem compelling, and our own experiments suggest that no such reactions occur on the time scale expected. Coulombic effects are expected, and can be demonstrated for the intra-monomer case. Analysis of titration curves suggests that coulombic interactions also occur across the dimer interface, as would be expected from simple physicochemical considerations.

Acknowledgments

We gratefully acknowledge support for the work reported here from grants NIH RO1 GM35438 (to ARC) and NIH RO1 GM62954 (to SAD).

References

[1] A. Osyczka, C.C. Moser, P.L. Dutton, Fixing the Q-cycle, Trends Biochem. Sci. 30 (2005) 176–182.
[2] A.R. Crofts, The cytochrome bc_1 complex — function in the context of structure, Annu. Rev. Physiol. 66 (2004) 689–733.
[3] A.R. Crofts, The bc_1 complex: what is there left to argue about? in: M. Wikström (Ed.), Biophysical and Structural Aspects of Bioenergetics, Royal Society of Chemistry Publishing, Cambridge, 2005, pp. 123–155.
[4] A.R. Crofts, Proton-coupled electron transfer at the Q_o-site of the bc_1 complex controls the rate of ubihydroquinone oxidation, Biochim. Biophys. Acta 1655 (2004) 77–92.
[5] A.R. Crofts, S. Lhee, S.B. Crofts, J. Cheng, S. Rose, Proton pumping in the bc_1 complex: a new gating mechanism that prevents short circuits, Biochim. Biophys. Acta 1757 (2006) 1019–1034.
[6] R. Covian, B.L. Trumpower, Rapid electron transfer between monomers when the cytochrome bc_1 complex dimer is reduced through center N, J. Biol. Chem. 280 (2005) 22732–22740.
[7] A. Osyczka, C.C. Moser, F. Daldal, P.L. Dutton, Reversible redox energy coupling in electron transfer chains, Nature 427 (2004) 607–612.
[8] C. Hunte, H. Palsdottir, B.L. Trumpower, Protonmotive pathways and mechanisms in the cytochrome bc_1 complex, FEBS Lett. 545 (2003) 39–46.
[9] A.Y. Mulkidjanian, Ubiquinol oxidation in the cytochrome b_1 complex: reaction mechanism and prevention of short-circuiting, Biochim. Biophys. Acta 1709 (2005) 5–34.
[10] A.Y. Mulkidjanian, Proton translocation by the cytochrome *bc*1 complexes of phototrophic bacteria: introducing the activated Q-cycle, Photochem. Photobiol. Sci. 6 (2007) 19–34.
[11] P.R. Rich, The quinone chemistry of *bc* complexes, Biochim. Biophys. Acta 1658 (2004) 165–171.
[12] A.R. Crofts, S.W. Meinhardt, K.R. Jones, M. Snozzi, The role of the quinone pool in the cyclic electron-transfer chain of *Rhodopseudomonas sphaeroides*: a modified Q-cycle mechanism, Biochim. Biophys. Acta 723 (1983) 202–218.
[13] A.R. Crofts, The Q-cycle, — a personal perspective, Photosynth. Res. 80 (2003) 223–243.
[14] V.P. Skulachev, Role of uncoupled and non-coupled oxidations in maintenance of safely low levels of oxygen and its one-electron reductants, Q. Rev. Biophys. 29 (1996) 169–202.
[15] A. Boveris, Determination of the production of superoxide radicals and hydrogen-peroxide in mitochondria, Methods Enzymol. 105 (1984) 429–435.
[16] J.F. Turrens, A. Alexandre, A.L. Lehninger, Ubisemiquinone is the electron donor for superoxide formation by complex III of heart mitochondria, Arch. Biochem. Biophys. 237 (1985) 408–414.
[17] F. Muller, The nature and mechanism of superoxide production by the electron transport chain: its relevance to aging, J. Am. Aging Assoc. 23 (2000) 227–253.
[18] J. Sun, B.L. Trumpower, Superoxide anion generation by the cytochrome *bc*1 complex, Arch. Biochem. Biophys. 419 (2003) 198–206.
[19] S. Raha, B.H. Robinson, Mitochondria, oxygen free radicals, and apoptosis, Am. J. Med. Genet. 106 (2001) 62–70.
[20] Q. Chen, E.J. Vazquez, S. Moghaddas, C.L. Hoppel, E.J. Lesnefsky, Production of reactive oxygen species by mitochondria: central role of complex III, J. Biol. Chem. 278 (2003) 36027–36031.
[21] B.S. Kristal, C.T. Jackson, H.Y. Chung, M. Matsuda, H.D. Nguyen, B.P. Yu, Defects at center P underlie diabetes-associated mitochondrial dysfunction, Free Radic. Biol. Med. 22 (1997) 823–833.
[22] N. Fisher, B. Meunier, The bc_1 complex: structure, function and dysfunction, in: J. Garcia-Trejo (Ed.), Recent Research Developments in Human Mitochondrial Myopathies, Research Signpost, India, 2002, pp. 97–112.
[23] N. Fisher, B. Meunier, Effects of mutations in mitochondrial cytochrome *b* in yeast and man — deficiency, compensation and disease, Eur. J. Biochem. 268 (2001) 1155–1162.
[24] A.R. Crofts, C.A. Wraight, The electrochemical domain of photosynthesis, Biochim. Biophys. Acta 726 (1983) 149–186.
[25] S.J. Hong, N. Ugulava, M. Guergova-Kuras, A.R. Crofts, The energy landscape for ubihydroquinone oxidation at the Q_o-site of the bc_1 complex in *Rhodobacter sphaeroides*, J. Biol. Chem. 274 (1999) 33931–33944.
[26] A.R. Crofts, Z. Wang, How rapid are the internal reactions of the ubiquinol: cytochrome *c*2 oxidoreductase? Photosynth. Res. 22 (1989) 69–87.
[27] D. Xia, C.-A. Yu, H. Kim, J.-Z. Xia, A.M. Kachurin, L. Zhang, L. Yu, J. Deisenhofer, Crystal structure of the cytochrome bc_1 complex from bovine heart mitochondria, Science 277 (1997) 60–66.
[28] Z. Zhang, L.-S. Huang, V.M. Shulmeister, Y.-I. Chi, K.-K. Kim, L.-W. Hung, A.R. Crofts, E.A. Berry, S.-H. Kim, Electron transfer by domain movement in cytochrome bc_1, Nature (Lond.) 392 (1998) 677–684.
[29] S. Iwata, J.W. Lee, K. Okada, J.K. Lee, M. Iwata, B. Rasmussen, T.A. Link, S. Ramaswamy, B.K. Jap, Complete structure of the 11-subunit bovine mitochondrial cytochrome bc_1 complex, Science 281 (1998) 64–71.
[30] C. Hunte, Insights from the structure of the yeast cytochrome bc_1 complex: crystallization of membrane proteins with antibody fragments, FEBS Lett. 504 (2001) 126–132.
[31] E.A. Berry, L.-S. Huang, L.K. Saechao, N.G. Pon, M. Valkova-Valchanova, F. Daldal, X-ray structure of *Rhodobacter capsulatus* cytochrome bc_1: comparison with its mitochondrial and chloroplast counterparts, Photosynth. Res. 81 (2004) 251–275.
[32] L. Esser, X. Gong, S. Yang, L. Yu, C.-A. Yu, D. Xia, Surface-modulated motion switch: capture and release of iron–sulfur protein in the cytochrome bc_1 complex, Proc. Natl. Acad. Sci. U. S. A. 103 (2006) 13045–13050.
[33] H. Palsdottir, C.G. Lojero, B.L. Trumpower, C. Hunte, Structure of the yeast cytochrome *bc*1 complex with a hydroxyquinone anion Qo site inhibitor bound, J. Biol. Chem. 278 (2003) 31303–31311.
[34] A.R. Crofts, B. Barquera, R.B. Gennis, R. Kuras, M. Guergova-Kuras, E.A. Berry, Mechanism of ubiquinol oxidation by the bc_1 complex: the different domains of the quinol binding pocket, and their role in mechanism, and the binding of inhibitors, Biochemistry 38 (1999) 15807–15826.
[35] A.R. Crofts, S. Hong, Z. Zhang, E.A. Berry, Physicochemical aspects of the movement of the Rieske iron sulfur protein during quinol oxidation by the bc_1 complex, Biochemistry 38 (1999) 15827–15839.
[36] S. Izrailev, A.R. Crofts, E.A. Berry, K. Schulten, Steered molecular dynamics simulation of the Rieske subunit motion in the cytochrome *bc*1 complex, Biophys. J. 77 (1999) 1753–1768.
[37] A.R. Crofts, V.P. Shinkarev, D.R.J. Kolling, S. Hong, The modified Q-cycle explains the apparent mismatch between the kinetics of reduction of cytochromes c_1 and b_H in the bc_1 complex, J. Biol. Chem. 278 (2003) 36191–36201.
[38] G. Engstrom, K. Xiao, C.-A. Yu, L. Yu, B. Durham, F. Millett, Photoinduced electron transfer between the Rieske iron–sulfur protein and cytochrome c_1 in the *Rhodobacter sphaeroides* cytochrome bc_1complex: effects of pH, temperature, and driving force, J. Biol. Chem. 277 (2002) 31072–31078.
[39] S. Rajagukguk, S. Yang, C.-A. Yu, L. Yu, B. Durham, F. Millett, Effect of mutations in the cytochrome *b ef* loop on the electron-transfer reactions of the Rieske iron–sulfur protein in the cytochrome bc_1 complex, Biochemistry 46 (2007) 1791–1798.
[40] A.R. Crofts, M. Guergova-Kuras, R. Kuras, N. Ugulava, J. Li, S. Hong, Proton-coupled electron transfer at the Q_o-site: what type of mechanism can account for the high activation barrier? Biochim. Biophys. Acta 1459 (2000) 456–466.
[41] X. Gao, X. Wen, L. Esser, B. Quinn, L. Yu, C.-A. Yu, D. Xia, Structural basis for the quinone reduction in the bc_1 complex: a comparative analysis of crystal structures of mitochondrial cytochrome bc_1 with bound substrate and inhibitors at the Q_i site, Biochemistry 42 (2003) 9067–9080.

[42] A.R. Crofts, V.P. Shinkarev, S.A. Dikanov, R.I. Samoilova, D. Kolling, Interactions of quinone with the iron–sulfur protein of the *bc*(1) complex: is the mechanism spring-loaded? Biochim. Biophys. Acta 1555 (2002) 48–53.

[43] R.I. Samoilova, D. Kolling, T. Uzawa, T. Iwasaki, A.R. Crofts, S.A. Dikanov, The interaction of the Rieske iron sulfur protein with occupants of the Q_o-site of the bc_1 complex, probed by 1D and 2D electron spin echo envelope modulation, J. Biol. Chem. 277 (2002) 4605–4608.

[44] Y. Zu, M.-J. Manon, M.M.-J. Couture, D.R.J. Kolling, A.R. Crofts, L.D. Eltis, J.A. Fee, J. Hirst, The reduction potentials of Rieske clusters: the importance of the coupling between oxidation state and histidine protonation state, Biochemistry 42 (2003) 12400–12408.

[45] N.B. Ugulava, A.R. Crofts, CD-monitored redox titration of the Rieske Fe–S protein of *Rhodobacter sphaeroides*: pH dependence of the mid-point potential in isolated bc_1 complex and in membranes, FEBS Lett. 440 (1998) 409–413.

[46] S.A. Dikanov, D.R.J. Kolling, B. Endeward, R.I. Samoilova, T.F. Prisner, S.K. Nair, A.R. Crofts, Identification of hydrogen bonds to the Rieske cluster through the weakly coupled nitrogens detected by electron spin echo envelope modulation spectroscopy, J. Biol. Chem. 281 (2006) 27416–27425.

[47] D.R.J. Kolling, J.S. Brunzelle, S. Lhee, A.R. Crofts, S.K. Nair, iron–sulfur protein of cytochrome bc_1 complex: exploring the roles of hydrogen bonding in tuning the redox potential of iron–sulfur clusters, Structure 15 (2007) 1–10.

[48] T. Iwasaki, A. Kounosu, D.R.J. Kolling, A.R. Crofts, S.A. Dikanov, A. Jin, T. Imai, A. Urushiyama, Characterization of the pH-dependent resonance Raman transitions of archaeal and bacterial Rieske [2Fe–2S] proteins, J. Am. Chem. Soc. 126 (2004) 4788–4789.

[49] T. Iwasaki, A. Kounosu, D.R.J. Kolling, S. Lhee, A.R. Crofts, S.A. Dikanov, T. Uchiyama, T. Kumasaka, H. Ishikawa, M. Kono, T. Imai, A. Urushiyama, Resonance Raman characterization of archaeal and bacterial Rieske protein variants with modified hydrogen bond network around the [2Fe–2S] center, Protein Sci. 15 (2006) 2019–2024.

[50] G.M. Ullmann, L. Noodleman, D.A. Case, Density functional calculation of p*K*a values and redox potentials in the bovine Rieske iron–sulfur protein, J. Biol. Inorg. Chem. 7 (2002) 632–639.

[51] C. Colbert, M.M.-J. Couture, L.D. Eltis, J.T. Bolin, A cluster exposed: structure of the Rieske ferredoxin from biphenyl dioxygenase and the redox properties of Rieske Fe–S proteins, Structure 8 (2000) 1267–1278.

[52] L.M. Hunsicker-Wang, A. Heine, Y. Chen, E.P. Luna, T. Todaro, Y.M. Zhang, P.A. Williams, D.E. McRee, J. Hirst, C.D. Stout, J.A. Fee, High-resolution structure of the soluble, respiratory-type Rieske protein from *Thermus thermophilus*: analysis and comparison, Biochemistry 42 (2003) 7303–7317.

[53] B.L. Trumpower, A concerted, alternating sites mechanism of ubiquinol oxidation by the dimeric cytochrome bc_1 complex, Biochim. Biophys. Acta 1555 (2002) 166–173.

[54] R.C. Sadoski, G. Engstrom, H. Tian, L. Zhang, C.A. Yu, L. Yu, B. Durham, F. Millett, Use of a photoactivated ruthenium dimer complex to measure electron transfer between the Rieske iron–sulfur protein and cytochrome c_1 in the cytochrome bc_1 complex, Biochemistry 39 (2000) 4231–4236.

[55] T.A. Link, The role of the "Rieske" iron sulfur protein in the hydroquinone oxidation (Q_p−) site of the cytochrome bc_1 complex: the "proton-gated affinity change" mechanism, FEBS Lett. 412 (1997) 257–264.

[56] E.A. Berry, L.S. Huang, Observations concerning the quinol oxidation site of the cytochrome bc_1 complex, FEBS Lett. 555 (2003) 13–20.

[57] T. Schröter, O.M. Hatzfeld, S. Gemeinhardt, M. Korn, T. Friedrich, B. Ludwig, T. Link, Mutational analysis of residues forming hydrogen bonds in the Rieske [2Fe2S] cluster of the cytochrome bc_1 complex of *Paracoccus denitrificans*, Eur. J. Biochem. 255 (1998) 100–106.

[58] E. Denke, T. Merbitzzahradnik, O.M. Hatzfeld, C.H. Snyder, T.A. Link, B.L. Trumpower, Alteration of the midpoint potential of the Rieske iron–sulfur protein by changes of amino acids forming H-bonds to the iron–sulfur cluster, J. Biol. Chem. 273 (1998) 9085–9093.

[59] M. Guergova-Kuras, R. Kuras, N. Ugulava, I. Hadad, A.R. Crofts, Specific mutagenesis of the Rieske iron sulfur protein in *Rhodobacter sphaeroides* shows that both thermodynamic gradient and the p*K* of the oxidized form determine the rate of quinol oxidation by the bc_1 complex, Biochemistry 39 (2000) 7436–7444.

[60] A.R. Crofts, S.J. Hong, N. Ugulava, B. Barquera, R.B. Gennis, M. Guergova-Kuras, E. Berry, Pathways for proton release during ubihydroquinone oxidation by the bc_1 complex, Proc. Natl. Acad. Sci. U. S. A. 96 (1999) 10021–10026.

[61] A. Crofts, M. Guergova-Kuras, N. Ugulava, R. Kuras, S. Hong, Proton processing at the Q_o-site of the bc_1 complex of *Rhodobacter sphaeroides*, Proc. XIIth Congress of Photosynthesis Research, Australia, Brisbane, 2002, p. 6.

[62] I.-J. Lin, Y. Chen, J.A. Fee, J. Song, W.M. Westler, J.L. Markley, Rieske protein from *Thermus thermophilus*: ^{15}N NMR titration study demonstrates the role of iron-ligated histidines in the pH dependence of the reduction potential, J. Am. Chem. Soc. 128 (2006) 10672–10673.

[63] M. Iwaki, G. Yakovlev, J. Hirst, A. Osyczka, P.L. Dutton, D. Marshall, P.R. Rich, Direct observation of redox-linked histidine protonation changes in the iron–sulfur protein of the cytochrome *bc*(1) complex by ATR-FTIR spectroscopy, Biochemistry 44 (2005) 4230–4237.

[64] M. Iwaki, A. Osyczka, C.C. Moser, P.L. Dutton, P.R. Rich, ATR-FTIR spectroscopy studies of iron–sulfur protein and cytochrome c_1 in the *Rhodobacter capsulatus* cytochrome bc_1 complex, Biochemistry 43 (2004) 9477–9486.

[65] C. Hunte, J. Koepke, C. Lange, T. Roβmanith, H. Michel, Structure at 2.3 Å resolution of the cytochrome bc_1 complex from the yeast *Saccharomyces cerevisiae* co-crystallized with an antibody F_v fragment, Structure 8 (2000) 669–684.

[66] A. Osyczka, H. Zhang, C. Mathé, P.R. Rich, C.C. Moser, P.L. Dutton, Role of the PEWY glutamate in hydroquinone–quinone oxidation-reduction catalysis in the Q_o site of cytochrome bc_1, Biochemistry 45 (2006) 10492–10503.

[67] T. Wenz, R. Covian, P. Hellwig, F. MacMillan, B. Meunier, B.L. Trumpower, C. Hunte, Mutational analysis of cytochrome *b* at the ubiquinol oxidation site of yeast complex III, J. Biol. Chem. 282 (2007) 3977–3988.

[68] N. Seddiki, B. Meunier, D. Lemesle-Meunier, G.I. Brasseur, Is cytochrome *b* glutamic acid 272 a quinol binding residue in the bc_1 complex of *Saccharomyces cerevisiae*? Biochemistry 47 (2008) 2357–2368.

[69] A.R. Klingen, H. Palsdottir, C. Hunte, G.M. Ullmann, Redox-linked protonation state changes in cytochrome bc_1 identified by Poisson–Boltzmann electrostatics calculations, Biochim. Biophys. Acta 1767 (2007) 204–221.

[70] I. Forquer, R. Covian, M.K. Bowman, B.L. Trumpower, D.M. Kramer, Similar transition states mediate the Q-cycle and superoxide production by the cytochrome bc_1 complex, J. Biol. Chem. 281 (2006) 38459–38465.

[71] J.L. Cape, M.K. Bowman, D.M. Kramer, A semiquinone intermediate generated at the Q_o site of the cytochrome bc_1 complex: importance for the Q-cycle and superoxide production, Proc. Natl. Acad. Sci. U. S. A. 104 (2007) 7887–7892.

[72] H. Zhang, A. Osyczka, P.L. Dutton, C.C. Moser, Exposing the complex III Q_o semiquinone radical, Biochim. Biophys. Acta 1767 (2007) 883–887.

[73] J. Zhu, T. Egawa, S.-R. Yeh, L. Yu, C.-A. Yu, Simultaneous reduction of iron–sulfur protein and cytochrome b_L during ubiquinol oxidation in cytochrome bc_1 complex, Proc. Natl. Acad. Sci. U. S. A. 104 (2007) 4864–4869.

[74] S. Junemann, P. Heathcote, P.R. Rich, On the mechanism of quinol oxidation in the bc_1 complex, J. Biol. Chem. 273 (1998) 21603–21607.

[75] S. De Vries, S.P.J. Albracht, J.A. Berden, C.A.M. Marres, E.C. Slater, The effect of pH, ubiquinone depletion and myxothiazol on the reduction kinetics of the prosthetic groups of QH_2:cytochrome *c* oxidoreductase, Biochim. Biophys. Acta 723 (1983) 91–103.

[76] D.R.J. Kolling, R.I. Samoilova, J.T. Holland, E.A. Berry, S.A. Dikanov, A.R. Crofts, Exploration of ligands to the Q_i-site semiquinone in the bc_1 complex using high resolution EPR, J. Biol. Chem. 278 (2003) 39747–39754.

[77] S. De Vries, J.A. Berden, E.C. Slater, Oxidation-reduction properties of an antimycin-sensitive semiquinone anion bound to QH_2:cytochrome *c* oxidoreductase, in: B.L. Trumpower (Ed.), Function of Quinones in Energy Conserving Systems, Academic Press, New York, 1982, pp. 235–246.

[78] D.E. Robertson, R.C. Prince, J.R. Bowyer, K. Matsuura, P.L. Dutton, T. Ohnishi, Thermodynamic properties of the semiquinone and its binding site in the ubiquinol:cytochrome *c* (c_2) oxidoreductase of respiratory and photosynthetic systems, J. Biol. Chem. 259 (1984) 1758–1763.

[79] A.R. Crofts, B. Barquera, G. Bechmann, M. Guergova, R. Salcedo-Hernandez, B. Hacker, S. Hong, R.B. Gennis, Structure and function in the bc_1 complex of *Rb. sphaeroides*, in: P. Mathis (Ed.), Photosynthesis: From Light to Biosphere, vol. II, Kluwer Academic Publ., Dordrecht, 1995, pp. 493–500.

[80] E.G. Glaser, S.W. Meinhardt, A.R. Crofts, Reduction of cytochrome b_{561} through the antimycin-sensitive site of the ubiquinol:cytochrome c_2 oxidoreductase complex of *Rps. sphaeroides*, FEBS Lett. 178 (1984) 336–342.

[81] S.W. Meinhardt, A.R. Crofts, A new effect of antimycin on the *b*-cytochromes of *Rps. sphaeroides*, in: C. Sybesma (Ed.), Advances in Photosynthesis Research, vol. 1, Martinus Nijhoff/Dr. W. Junk Publishers, The Hague, 1984, pp. 649–652.

[82] J.C. Salerno, Y. Xu, P. Osgood, K.C.H., T.E. King, Thermodynamic and spectroscopic characteristics of the cytochrome bc_1 complex. Role of quinone in the behavior of cytochrome b_{562}, J. Biol. Chem. 264 (1989) 15398–15403.

[83] J.C. Salerno, M. Osgood, Y. Liu, H. Taylor, C.P. Scholes, Electron nuclear double resonance (ENDOR) of the Q_c-ubiSQ radical in the mitochondrial electron transport chain, Biochemistry 29 (1990) 6987–6993.

[84] S.A. Dikanov, R.I. Samoilova, D.R.J. Kolling, J.T. Holland, A.R. Crofts, Hydrogen bonds involved in binding the Q_i-site semiquinone in the bc_1 complex, identified through deuterium exchange using pulsed EPR, J. Biol. Chem. 279 (2004) 15814–15823.

[85] P.R. Rich, A.E. Jeal, S.A. Madgwick, A.J. Moody, Inhibitor effects on redox-linked protonations of the *b* hemes of the mitochondrial bc_1 complex, Biochim. Biophys. Acta 1018 (1990) 29–40.

[86] L.S. Huang, D. Cobessi, E.Y. Tung, E.A. Berry, Binding of the respiratory chain inhibitor antimycin to the mitochondrial bc_1 complex: a new crystal structure reveals an altered intramolecular hydrogen-bonding pattern, J. Mol. Biol. 351 (2005) 573–597.

[87] L. Esser, M. Elberry, F. Zhou, C.-A. Yu, L. Yu, D. Xia, Inhibitor complexed structures of the cytochrome bc_1 complex from the photosynthetic bacterium *Rhodobacter sphaeroides*, J. Biol. Chem. 283 (2008) 2846–2857.

[88] O. Carugo, K.D. Carugo, When X-rays modify the protein structure: radiation damage at work, Trends Biochem. Sci. 30 (2005) 213–219.

[89] M.S. Weiss, et al., On the influence of the incident photon energy on the radiation damage in crystalline biological samples, J. Synchrotron Radiat. 12 (2005) 304–309.

[90] S.A. Dikanov, J.T. Holland, B. Endeward, D.R.J. Kolling, R.I. Samoilova, T.F. Prisner, A.R. Crofts, Hydrogen bonds between nitrogen donors and the semiquinone in the Q_i-site of the bc_1 complex, J. Biol. Chem. 282 (2007) 25831–25841.

[91] P.L. Dutton, J.B. Jackson, Thermodynamic and kinetics characterization of electron-transfer components *in situ* in *Rps. spheroides* and *Rhodospirillum rubrum*, Eur. J. Biochem. 30 (1972) 495–510.

[92] P.L. Dutton, D.M. Wilson, Redox potentiometry in biological systems, Methods Enzymol. 54 (1976) 411–435.

[93] K.M. Andrews, Purification and characterization of the cytochrome bc_1 complex from *Rhodobacter sphaeroides*. Ph.D. Thesis, University of Illinois at Urbana-Champaign., 1984.

[94] A.R. Crofts, B. Barquera, G. Bechmann, M. Guergova, R. Salcedo-Hernandez, B. Hacker, S. Hong, R.B. Gennis, Structure and function in the bc_1-complex of *Rb. sphaeroides*, in: P. Mathis (Ed.), Photosynthesis: From Light to Biosphere, vol. II, Kluwer Academic Publ., Dordrecht, 1995, pp. 493–500.

[95] D. Robertson, R. Prince, J. Bowyer, K. Matsuura, P. Dutton, T. Ohnishi, Thermodynamic properties of the semiquinone and its binding site in the ubiquinol-cytochrome *c* (c2) oxidoreductase of respiratory and photosynthetic systems, J. Biol. Chem. 259 (1984) 1758–1763.
[96] P.R. Rich, A.E. Jeal, S.A. Madgwick, A.J. Moody, Inhibitor effects on redox-linked protonations of the *b* haems of the mitochondrial *bc*1 complex, Biochim. Biophys. Acta 1018 (1990) 29–40.
[97] A. Zweck, G. Bechmann, H. Weiss, The pathway of the quinol/quinone transhydrogenation reaction in ubiquinol: cytochrome-*c* reductase of *Neurospora* mitochondria, Eur. J. Biochem. 183 (1989) 199–203.
[98] P.R. Rich, S.A. Madgwick, D.A. Moss, The interactions of duroquinol, DBMIB and NQNO with the chloroplast cytochrome *bf* complex, Biochim. Biophys. Acta 1058 (1991) 312–328.
[99] V.P. Shinkarev, A.R. Crofts, C.A. Wraight, The electric field generated by photosynthetic reaction center induces rapid reversed electron transfer in the *bc*(1) complex, Biochemistry 40 (2001) 12584–12590.
[100] J.N. Siedow, S. Power, F.F. del la Rosa, G. Palmer, The preparation and characterization of highly purified enzymically active complex III from baker's yeast, J. Biol. Chem. 253 (1978) 2392–2399.
[101] F.F. de la Rosa, G. Palmer, Reductive titration of CoQ-depleted complex III from baker's yeast: evidence for an exchange-coupled complex between QHand low-spin ferricytochrome *b*, FEBS Lett. 163 (1983) 140–143.
[102] J.W. Cooley, T. Ohnishi, F. Daldal, Binding dynamics at the quinone reduction (Q_i) site influence the equilibrium interactions of the iron sulfur protein and hydroquinone oxidation (Q_o) site of the cytochrome bc_1 complex. Biochemistry 44 (2005) 10520–10532.
[103] C.-A. Yu, X. Wen, K. Xiao, D. Xia, L. Yu, Inter- and intra-molecular electron transfer in the cytochrome bc_1 complex, Biochim. Biophys. Acta 1555 (2002) 65–70.
[104] X. Gong, L. Yu, D. Xia, C.-A. Yu, Evidence for electron equilibrium between the two hemes b_L in the dimeric cytochrome bc_1 complex, J. Biol. Chem. 280 (2005) 9251–9257.
[105] A.R. Crofts, E.A. Berry, Structure and function of the cytochrome bc_1 complex of mitochondria and photosynthetic bacteria, Curr. Opin. Struct. Biol. 8 (1998) 501–509.
[106] E. Berry, M. Guergova-Kuras, L.-S. Huang, A.R. Crofts, Structure and function of cytochrome *bc* complexes, Annu. Rev. Biochem. 69 (2000) 1007–1077.
[107] J.R. Bowyer, A.R. Crofts, On the mechanism of photosynthetic electron transfer in *Rps. capsulata* and *Rps. sphaeroides*, Biochim. Biophys. Acta 636 (1981) 218–233.
[108] S.W. Meinhardt, A.R. Crofts, Kinetic and thermodynamic resolution of cytochrome c_1 and cytochrome c_2 from *Rps. sphaeroides*, FEBS Lett. 149 (1982) 223–227.
[109] S.W. Meinhardt, A.R. Crofts, The role of cytochrome b_{566} in the electron transfer chain of *Rps. sphaeroides*, Biochim. Biophys. Acta 723 (1983) 219–230.
[110] M. Snozzi, A.R. Crofts, Electron transport in chromatophores from *Rhodopseudomonas sphaeroides* GA fused with liposomes, Biochim. Biophys. Acta, Bioenerg. 766 (1984) 451–463.
[111] V.P. Shinkarev, A.R. Crofts, C.A. Wraight, Spectral analysis of the bc_1 complex components *in Situ*: beyond the traditional difference approach, Biochim. Biophys. Acta 1757 (2005) 67–77.
[112] V.P. Shinkarev, A.R. Crofts, C.A. Wraight, *In situ* kinetics of cytochromes c_1 and c_2, Biochemistry 45 (2006) 7897–7903.
[113] V.P. Shinkarev, A.R. Crofts, C.A. Wraight, Spectral and kinetic resolution of the bc_1 complex components *in situ*: a simple and robust alternative to the traditional difference wavelength approach, Biochim. Biophys. Acta 1757 (2006) 273–283.
[114] R. Fato, M. Battino, M. Degli Esposti, G. Parenti Castelli, G. Lenaz, Determination of partition and lateral diffusion coefficients of ubiquinones by fluorescence quenching of n-(9-anthroyloxy)stearic acids in phospholipid vesicles and mitochondrial membranes, Biochemistry 25 (1986) 3378–3390.
[115] J.L. Cape, J.R. Strahan, M.J. Lenaeus, B.A. Yuknis, T.T. Le, J.N. Shepherd, M.K. Bowman, D.M. Kramer, The respiratory substrate rhodoquinol induces Q-cycle bypass reactions in the yeast cytochrome bc_1 complex — mechanistic and physiological implications, J. Biol. Chem. 280 (2005) 34654–34660.
[116] J.S. Rieske, H. Baum, C.D. Stoner, S.H. Lipton, On the antimycin-sensitive cleavage of complex III of the mitochondrial respiratory chain, J. Biol. Chem. 242 (1967) 4854–4866.
[117] A.R. Crofts, E.A. Berry, Structure and function of the cytochrome bc_1 complex of mitochondria and photosynthetic bacteria, Curr. Opin. Struct. Biol. 8 (1998) 501–509.
[118] R.A. Marcus, N. Sutin, Electron transfers in chemistry and biology, Biochim. Biophys. Acta 811 (1985) 265–322.
[119] D. DeVault, Quantum mechanical tunnelling in biological systems, Q. Rev. Biophys. 13 (1980) 387–564.
[120] C.C. Moser, C.C. Page, R. Farid, P.L. Dutton, Biological electron transfer, J. Bioenerg. Biomembranes 27 (1995) 263–274.
[121] C.C. Moser, C.C. Page, X.X. Chen, P.L. Dutton, Biological electron tunnelling through protein media, J. Biol. Inorg. Chem. 2 (1997) 393–398.
[122] C.C. Moser, T.A. Farid, S.E. Chobot, P.L. Dutton, Electron tunnelling chains of mitochondria, Biochim. Biophys. Acta 1757 (2006) 1096–1109.
[123] C.C. Moser, J.M. Keske, K. Warncke, R.S. Farid, P.L. Dutton, Nature of biological electron transfer, Nature 355 (1992) 796.
[124] C.C. Moser, C.C. Page, P.L. Dutton, Darwin at the molecular scale: selection and variance in electron tunnelling proteins including cytochrome *c* oxidase, Philos. Trans. R. Soc. 361 (2006) 1295–1305.
[125] V.P. Shinkarev, C.A. Wraight, Intermonomer electron transfer in the bc_1 complex dimer is controlled by the energized state and by impaired electron transfer between low and high potential hemes, FEBS Lett. 581 (2007) 1535–1541.
[126] R. Covián, J.P. Juan Pablo Pardo, R. Moreno-Sánchez, Tight binding of inhibitors to bovine bc_1 complex is independent of the Rieske protein redox state — consequences for semiquinone stabilization in the quinol oxidation site, J. Biol. Chem. 277 (2002) 48449–48455.
[127] A.R. Crofts, The Q-cycle, — a personal perspective, Photosynth. Res. 80 (2003) 223–243.
[128] A. Kröger, M. Klingenberg, The kinetics of the redox reactions of ubiquinone related to the electron-transport activity in the respiratory chain, Eur. J. Biochem. 34 (1973) 358–368.
[129] A. Kröger, M. Klingenberg, Further evidence for the pool function of ubiquinone as derived from the inhibition of the electron transport by antimycin, Eur. J. Biochem. 39 (1973) 313–323.
[130] J. Fernandez-Velasco, A.R. Crofts, Complexes or super complexes: inhibitor titrations show that electron transfer in chromatophores from *Rb. sphaeroides* involves a dimeric ubiquinol: cytochrome c_2 oxidoreductase, and is delocalized, Biochem. Soc. Trans. 19 (1991) 588–593.
[131] G. Bechmann, H. Weiss, P. Rich, Nonlinear inhibition curves for tight-binding inhibitors of dimeric ubiquinol-cytochrome *c* oxidoreductase — evidence for rapid inhibitor mobility, Eur. J. Biochem. 208 (1992) 315–325.
[132] R.C. Prince, P.L. Dutton, Single and multiple turnover reactions in the ubiquinone-cytochrome b–c_2 oxidoreductase of *Rhodopseudomonas sphearoides*: the physical chemistry of the major electron donor to cytochrome c_2, and its coupled reactions, Biochim. Biophys. Acta 462 (1977) 731–747.
[133] G. Venturoli, M. Virgili, B.A. Melandri, A.R. Crofts, Kinetic measurements of electron transfer in coupled chromatophores from photosynthetic bacteria: a method of correction for the electrochromic effects, FEBS Lett. 219 (1987) 477–484.
[134] G. Venturoli, J.G. Fernandez-Velasco, A.R. Crofts, B.A. Melandri, The effect of the size of the quinone pool on the electrogenic reactions in the UQH_2:cyt c_2 oxidoreductase of *Rhodobacter capsulatus*. Pool behavior at the quinone reductase site, Biochim. Biophys. Acta 935 (1988) 258–272.
[135] G. Venturoli, J.G. Fernandez-Velasco, A.R. Crofts, B.A. Melandri, Demonstration of a collisional interaction of ubiquinol with the ubiquinol-cytochrome c_2 oxidoreductase complex in chromatophores from *Rhodobacter sphaeroides*, Biochim. Biophys. Acta, Bioenerg. 851 (1986) 340–352.
[136] R. Kuras, M. Guergova-Kuras, A.R. Crofts, Steps toward constructing a cytochrome b_6f complex in the purple bacteria *Rhodobacter sphaeroides*: an example of the structural plasticity of a membrane cytochrome, Biochemistry 37 (1998) 16280–16288.
[137] A.R. Crofts, S. Rose, Marcus treatment of endergonic reactions: a commentary, Biochim. Biophys. Acta 1767 (2007) 1228–1232.
[138] A. Kuki, P.G. Wolynes, Electron tunneling paths in proteins, Science 236 (1987) 1647–1652.
[139] I.A. Balabin, J.N. Onuchic, Dynamically controlled protein tunneling paths in photosynthetic reaction centers, Science 290 (2000) 114–117.
[140] T. Kawatsu, D.N. Beratan, T. Kakitani, Conformationally averaged score functions for electronic propagation in proteins, J. Phys. Chem. B 110 (2006) 5747–5757.
[141] T.R. Prytkova, I.V. Kurnikov, D.N. Beratan, Coupling coherence distinguishes structure sensitivity in protein electron transfer, Science 315 (2007) 622–625.
[142] B.M. Hoffman, L.M. Celis, D.A. Cull, A.D. Patel, J.L. Seifert, K.E. Wheeler, J. Wang, J. Yao, I.V. Kurnikov, J.M. Nocek, Differential influence of dynamic processes on forward and reverse electron transfer across a protein–protein interface, Proc. Natl. Acad. Sci. U. S. A. 102 (2005) 3564–3569.
[143] H. Nishioka, A. Kimura, T. Yamato, T. Kawatsu, T. Kakitani, Interference, fluctuation, and alternation of electron tunneling in protein media. 1. two tunneling routes in photosynthetic reaction center alternate due to thermal fluctuation of protein conformation, J. Phys. Chem. B 109 (2005) 1978–1987.
[144] F.A. Walker, Magnetic spectroscopic (EPR, ESEEM, Mössbauer, MCD and NMR) studies of low-spin ferriheme centers and their corresponding heme proteins, Coord. Chem. Rev. 185–186 (1999) 471–534.
[145] F.A. Walker, Models of the bis-histidine-ligated electron-transferring cytochromes. Comparative geometric and electronic structure of low-spin ferro- and ferrihemes, Chem. Rev. 104 (2004) 589–615.
[146] C.-H. Yun, A.R. Crofts, R.B. Gennis, Assignment of the histidine axial ligands to the cytochrome b_H and cytochrome b_L components of the bc_1 complex from *Rb. sphaeroides* by site-directed mutagenesis, Biochemistry 30 (1991) 6747–6754.
[147] J.T. Holland, Investigation of the interaction between cytochrome b_H and the Q_i-site in *Rhodobacter sphaeroides*, Center for Biophysics and Computational Biology, vol. Ph. D. University of Illinois, Urbana-Champaign, 2007, p. 163.
[148] U. Brandt, J.G. Okun, Role of deprotonation events in ubihydroquinone:cytochrome *c* oxidoreductase from bovine heart and yeast mitochondria, Biochemistry 36 (1997) 11234–11240.